Paleomagnetic evidence for a large rotation of the Yukon block relative to Laurentia: Implications for a low-latitude Sturtian glaciation and the breakup of Rodinia

Athena E. Eyster[1,†], Roger R. Fu[2], Justin V. Strauss[3], Benjamin P. Weiss[2], Charlie F. Roots[4,§], Galen P. Halverson[5], David A.D. Evans[6], and Francis A. Macdonald[1]

[1]*Department of Earth and Planetary Sciences, Harvard University, 20 Oxford Street, Cambridge, Massachusetts 02138, USA*
[2]*Department of Earth, Atmospheric and Planetary Sciences, Massachusetts Institute of Technology, Building 54-724, Cambridge, Massachusetts 02139, USA*
[3]*Department of Earth Sciences, Dartmouth College, HB6105 Fairchild Hall, Hanover, New Hampshire 03755, USA*
[4]*Natural Resources Canada, c/o Box 2703, K-102, Whitehorse, Yukon Y1A 2C6, Canada*
[5]*Department of Earth and Planetary Sciences, McGill University, 3450 University Street, Montréal, Québec H3A0E8, Canada*
[6]*Department of Geology and Geophysics, Yale University, New Haven, Connecticut 06520, USA*

ABSTRACT

Understanding the tectonic history of the supercontinent Rodinia is crucial for testing proposed links among Neoproterozoic tectonics, supercontinent cycles, climate, and biogeochemistry. The Neoproterozoic Mount Harper volcanics of the Ogilvie Mountains, Yukon, Canada, interfinger with Sturtian-age (ca. 717–660 Ma) glacial deposits that were deposited in narrow, fault-bounded basins related to the breakup of Rodinia. Here, we present new paleomagnetic data from the Mount Harper volcanics and isolate four paleomagnetic directions: a low-temperature direction recording the present geomagnetic field, a mid-temperature direction consistent with a Cretaceous overprint, and two high-temperature directions, one of which is carried by hematite and likely represents a chemical overprint, and the other of which is carried by magnetite and likely is a primary direction. This primary pole passes the fold and conglomerate tests and includes a reversal but is 50° away from the coeval 721–712 Ma Laurentian Franklin large igneous province pole. This difference can be reconciled using a 50° counterclockwise rotation of the Yukon block relative to Laurentia. The prerotation reconstruction of the Yukon block relative to Laurentia aligns Neoproterozoic fault orientations and facies belts between the Wernecke and Mackenzie Mountains, rectifies paleoflow measurements in Mesoproterozoic and Paleoproterozoic strata, and realigns the orientation of the ca. 1260 Ma Bear River dikes with the Mackenzie dike swarm of northern Canada. This reconstruction also facilitates future studies that relate Neoproterozoic sedimentary and structural patterns to the fragmentation of Rodinia. Finally, this low-latitude pole supports the snowball Earth interpretation of the ca. 717 Ma Sturtian glacial deposits.

INTRODUCTION

The protracted breakup of the supercontinent Rodinia has long been associated with Neoproterozoic environmental and biological change (Kirschvink, 1992; Hoffman and Schrag, 2002; Goddéris et al., 2003). However, the age, geometry, configuration, and kinematics of Rodinia's fragmentation remain poorly constrained. Because Neoproterozoic-Cambrian strata on the margins of Laurentia are interpreted as passive margin sequences (Hoffman, 1991), many paleogeographic reconstructions place it at the core of Rodinia (e.g., Li et al., 2008). Due to this central location, studies of Laurentian basins can assist in understanding the breakup of Rodinia (e.g., Ross, 1991; Macdonald et al., 2012; Strauss et al., 2015). Several discrete extensional events on the western margin of Laurentia have been attributed to the rifting of Rodinia, implying a prolonged and complex breakup history. Early Neoproterozoic (ca. 1.2–0.78 Ga Sequence B of Young et al., 1979) sedimentary successions were interpreted as recording basin-forming events consistent with a NNW-facing margin in present coordinates (Aitken, 1981).

Alternatively, Turner and Long (2008) argued for NE-SW extension on the western margin of Laurentia based on the interpretation of multiple NE-SW–oriented structures in the Mackenzie Mountains as transfer faults. In addition to these older structures, which can be interpreted as recording early Neoproterozoic rifting, late Neoproterozoic rifting (Windermere Supergroup and Sequence C of Young et al., 1979) is thought to have occurred during two separate intervals: ca. 780–660 Ma (Jefferson and Parrish, 1989; Mustard, 1991) and ca. 580–560 Ma in the southern Cordillera (Colpron et al., 2002; Lund, 2008; Lund et al., 2010; Yonkee et al., 2014).

There are numerous candidates for the continents that rifted away from Laurentia's northern and western margins, including Antarctica, Australia, South China, North China, Siberia, and West Africa (Sears and Price, 1978; Moores, 1991; Hoffman, 1991; Dalziel, 1997; Sears and Price, 2003; Pisarevsky et al., 2003; Li et al., 2008; Evans, 2009; Fu et al., 2015; Ernst et al., 2016). Irrespective of the identity of its former conjugate partners in Rodinia, Yukon records the Neoproterozoic tectonic evolution of both the northern and western margins of Laurentia (e.g., Thorkelson et al., 2005; Macdonald et al., 2012; Strauss et al., 2015), and it is a keystone for future attempts to elucidate the extensional history in this part of Rodinia.

Recent geochronological data from Neoproterozoic sedimentary successions in Yukon enable more accurate constraints on basin-forming events in Laurentia during the early fragmentation of Rodinia. In the Coal Creek inlier of west-central Yukon (Figs. 1 and 2), early Neoproterozoic synsedimentary faulting and
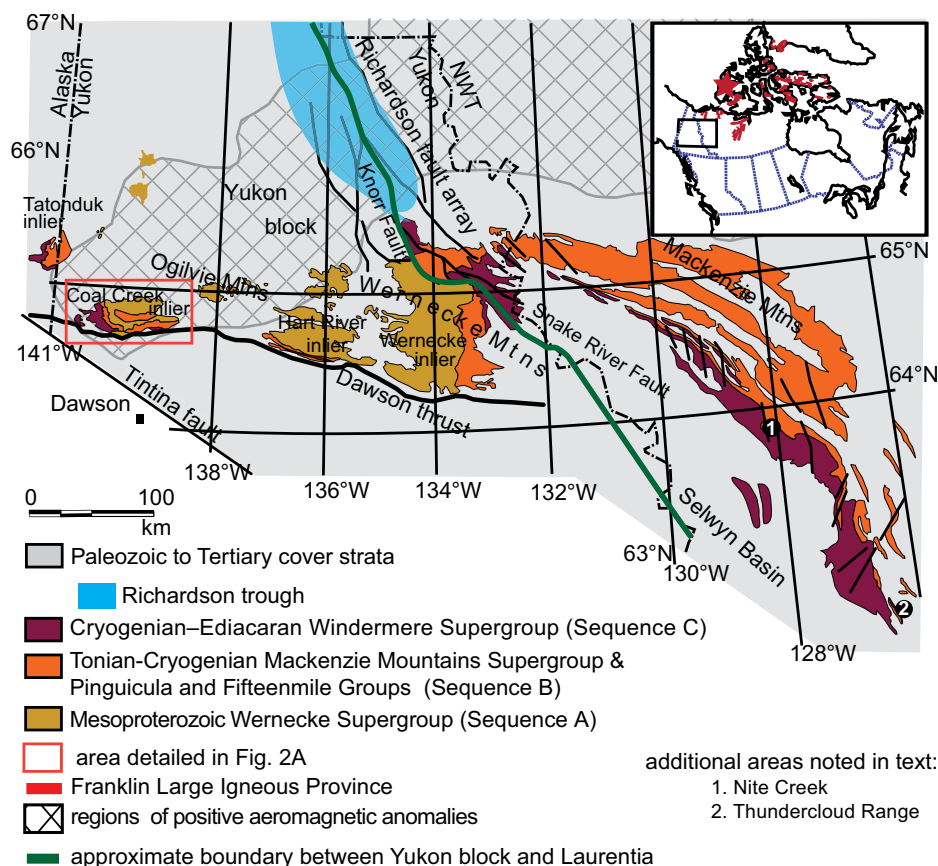
---

†aeyster@fas.harvard.edu
§Deceased.

Figure 1. Map of northwest Canada with Proterozoic inliers. Note Richardson trough (after Morrow, 1999) and Richardson fault array separate the Tatonduk, Coal Creek, Hart River, and Wernecke inliers from the Mackenzie Mountains. The cross-hatched areas indicate aeromagnetic highs following Aspler et al. (2003) and Pilkington and Saltus (2009). The solid green line depicts approximate boundary between the Yukon block and Laurentia. Inset depicts the extent of the Franklin large igneous province (red; Buchan and Ernst, 2004, 2013; Buchan et al., 2010). NWT—Northwest Territories.

Paleozoic, or Neoproterozoic age. In addition, Park et al. (1992) acknowledged that their results were inconclusive due to limited sampling, and that additional sampling and examination were needed to validate or refute them. Here, we present new paleomagnetic results from the Mount Harper volcanics that resolve these uncertainties, allowing us to infer the geometry of Neoproterozoic synsedimentary structures relative to the Laurentian craton and relative motions during the breakup of Rodinia, and additionally, to explore the paleomagnetic constraints on the ca. 717 Ma Yukon glacial deposits that may record the initiation of snowball Earth glaciation on Laurentia.

GEOLOGICAL SETTING

The Yukon block (Jeletsky, 1962) is a crustal fragment separated from contiguous Laurentia to the east by the Richardson trough and the Richardson fault array (Fig. 1). The Richardson trough represents a Cambrian–Devonian deep-water basin formed above a failed rift arm between the Yukon block and Mackenzie Platform (Gabrielse, 1967; Pugh, 1983; Norris, 1985; Cecile et al., 1997; Morrow, 1999; Rohr et al., 2011). The Richardson fault array is a regional-scale fault system with a history of reactivation that has controlled sedimentation and deformation in the area since its inception in the Proterozoic (Eisbacher, 1981, 1983; Norris, 1985, 1997; Abbott, 1996, 1997; Crawford et al., 2010; Rohr et al., 2011). Proterozoic strata in the Yukon block consist of three major successions (Young et al., 1979) exposed in four inliers: the Tatonduk, Coal Creek, Hart River, and Wernecke inliers (Fig. 1). The oldest rocks consist of Sequence A, a polydeformed succession of mixed carbonate and siliciclastic strata of the late Paleoproterozoic–early Mesoproterozoic Wernecke Supergroup (Delaney, 1981; Thorkelson et al., 2005; Furlanetto et al., 2013). Sequence B includes the Pinguicula, Hematite Creek, and Fifteenmile Groups in the Yukon block inliers. These groups are correlative with the Mackenzie Mountains Supergroup, which constitutes the oldest strata found in the Mackenzie Mountains to the east. A tuff in the Fifteenmile Group of the Coal Creek inlier has been dated at 811.51 ± 0.25 Ma (U-Pb isotope dilution–thermal ionization mass spectrometry [ID-TIMS] on zircon; Macdonald et al., 2010). Sequence C includes the Cryogenian–Ediacaran–aged strata of the Windermere Supergroup.

The focus of this study is the Coal Creek inlier, in the south-central Ogilvie Mountains (Figs. 1 and 2). In this area, the Mount Harper Group forms the base of the Windermere Super-

subsidence have been linked to extension on the northern margin of Laurentia (Macdonald et al., 2012). In contrast, the later Neoproterozoic Mount Harper Group was deposited in a volcanically active half graben previously attributed to extension or transtension along the western margin of Laurentia (Mustard, 1991; Mustard and Roots, 1997; Strauss et al., 2015). Recent geochronological and geochemical data from the Mount Harper volcanics of the upper Mount Harper Group (Macdonald et al., 2010; Cox et al., 2013) highlight connections with igneous activity associated with the Franklin large igneous province (LIP; Heaman et al., 1992; Denyszyn et al., 2009a, 2009b), which has yielded a robust, low-latitude, grand-mean paleomagnetic pole (Fahrig et al., 1971; Robertson and Baragar, 1972; Fahrig and Schwarz, 1973; Palmer and Hayatsu, 1975; Park, 1981; Christie and Fahrig, 1983; Palmer et al., 1983; Heaman et al., 1992; Pehrsson and Buchan, 1999; Buchan

et al., 2000; Denyszyn et al., 2009a, 2009b). Taken at face value, these data connect extension or transtension recorded in Yukon with the paleogeography of Laurentia relative to the other cratons in Rodinia. Moreover, the link between the ca. 717 Ma onset of the Sturtian glaciation in Yukon and the low-latitude paleomagnetic pole of the Franklin LIP is a key line of evidence for snowball Earth (Macdonald et al., 2010). The similarity in ages and robust Franklin paleomagnetic pole provide a unique opportunity to better understand the Sturtian glaciation and identify tectonic movements of the Yukon block relative to the Laurentian craton using paleomagnetism.

A previous reconnaissance-level paleomagnetic study of the Mount Harper volcanics suggested a pole distinct from the Franklin grand-mean pole (Park et al., 1992); however, it was unclear if this difference was due to large true polar wander, anomalous magnetic field behavior, or a tectonic rotation of Cretaceous,
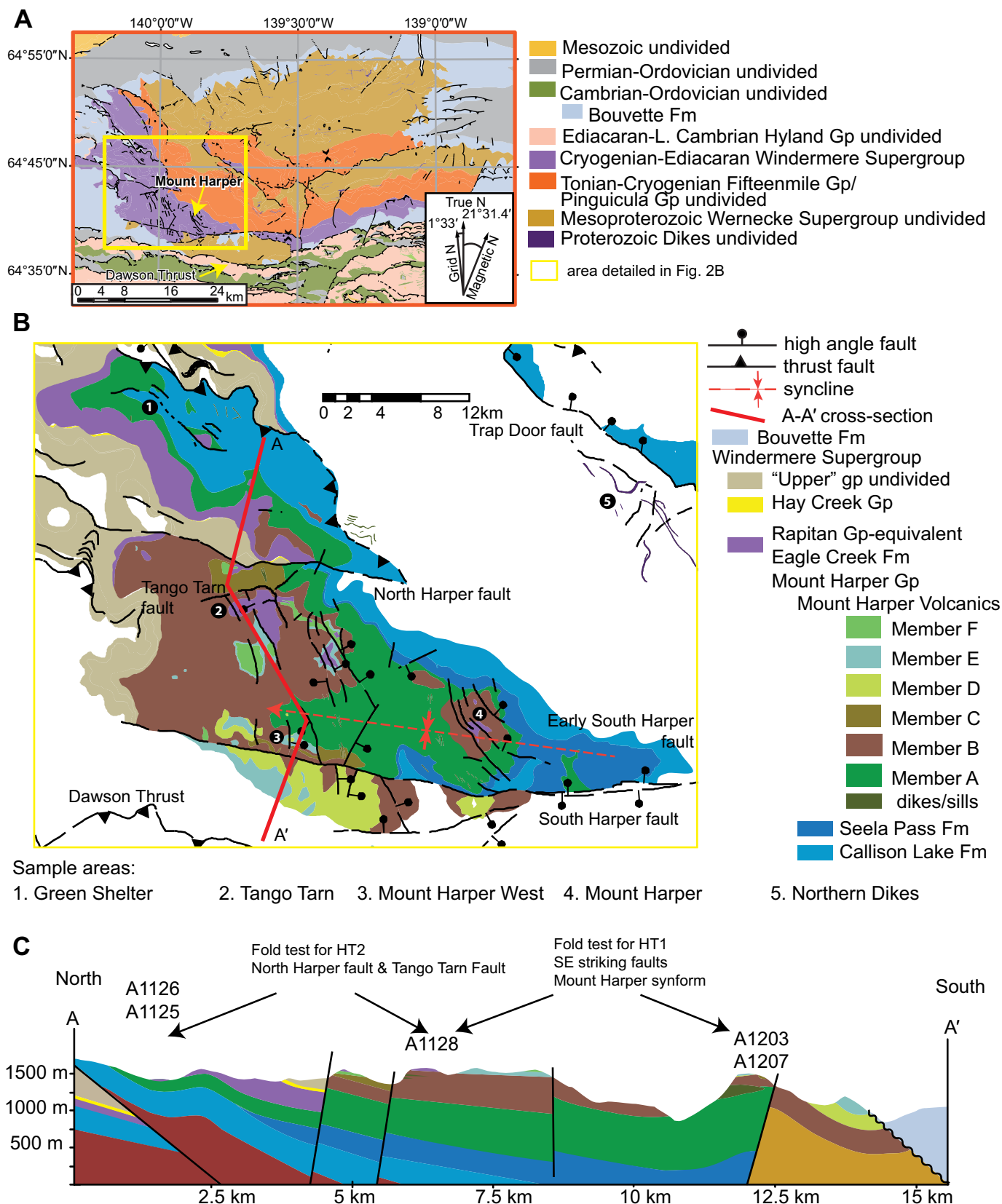
Figure 2. (A) Map of the Coal Creek inlier (modified from Strauss et al., 2014b). (B) Focus on the Mount Harper Group with the Mount Harper volcanics divided into informal members. Important sample areas and cross-section line A-A′ are indicated on map. (C) Cross-section A-A′ across the Mount Harper volcanics.

group and includes, in stratigraphically ascending order, the ca. 755–735 Ma Callison Lake Formation (Strauss et al., 2014a, 2015; Rooney et al., 2015), the Seela Pass Formation, and the Mount Harper volcanics (Mustard, 1991; Mustard and Roots, 1997; Macdonald et al., 2010, 2011; Strauss et al., 2014b, 2015). The Callison Lake and Seela Pass Formations record fault-related carbonate and siliciclastic sedimentation associated with early phases of Neoproterozoic extension in NW Canada (Mustard, 1991; Mustard and Roots, 1997; Strauss et al., 2015).

The Mount Harper volcanics consist of a bimodal magmatic suite that is divided into six informal members along with intrusive domes and dikes (Figs. 2 and 3; Mustard and Roots, 1997). Geochemically, the total alkali-FeO-MgO (AFM) projection shows samples on both sides of the tholeiitic/calc-alkaline divide (Mustard and Roots, 1997; Cox, 2015). This is unusual, because, at the same time, the close association of the volcanics with normal faulting and extensional activity indicates a relationship between extension and volcanism (Mustard and Roots, 1997). The existence of magmas with calc-alkaline affinities but connected to lithospheric extension rather than subduction has been documented in the North American Pacific Northwest and Basin and Range (Robyn, 1979; Gans et al., 1989; Smith et al., 1990; Hooper et al., 1995; Hawkesworth et al., 1995; Morris et al., 2000; Camp et al., 2003), as well as in eastern Queensland, Australia (Ewart et al., 1992), and northeastern China (Fan et al., 2003). In such cases, it is suggested that the rift-related calc-alkaline magmatism can be explained by extension-related decompression melting of subcontinental crust or mantle that was previously hydrated and enriched by earlier subduction events, rather than by contemporaneous subduction. The basaltic lower suite consists of members A, B, and C, and the more felsic upper suite is composed of members D, E, and F (Mustard and Roots, 1997). Local evidence of soft sediment deformation in the Seela Pass units beneath the basal pillow basalt flows of member A (Fig. 3) suggests these units were unlithified during emplacement of the volcanics (Mustard and Roots, 1997). Member A consists of pillowed and minor massive flows, and member B consists of basaltic flows composed of two facies: a pillow-dominated chloritic facies and an overlying hematitic and highly vesiculated unit with pahoehoe flow tops (Fig. 3). The transition between these members was originally defined in reference sections based on chemical analysis (Mustard and Roots, 1997). For the hematitic facies, it is likely that iron oxidation of subaerially erupted basalts resulted in the growth of synvolcanic hematite (Mustard and Roots,

1997; Roots, 1987). Fine- to medium-grained chloritic and SE-trending diabase dikes and sills are associated with members A and B (Mustard and Roots, 1997), and the dikes may have fed the extrusive member B volcanics. Member B is disconformably overlain by various members of the upper Mount Harper volcanics and Rapitan Group–equivalent strata of the Eagle Creek formation (Mustard and Roots, 1997; Strauss et al., 2014b). Member C consists predominantly of basaltic pyroclastic to epiclastic breccias, whereas member D is rhyolitic in composition and locally dominated by massive columnar-jointed flows that weather light pink to gray-green (Fig. 3). A thin crystal tuff layer marks the upper contact of member D in two places. Member E is composed primarily of dark-blue chlorite-bearing andesitic flows, tuffs, and breccias (Mustard and Roots, 1997). Pillowed flows up to 20 m thick are found in member E, as well as local subaerial pahoehoe textures (Fig. 3). Three mounds of silicic rubble, thought to be ancient rhyolite domes, are locally centered on feeder dikes and appear to be younger than the rest of member D, because they intrude member E (Mustard and Roots, 1997). These rhyolite domes were dated with U-Pb chemical-abrasion (CA) ID-TIMS on zircon at 717.43 ± 0.14 Ma (Macdonald et al., 2010). Member F is the youngest of the rocks in the Mount Harper volcanics and includes intermediate to mafic flows, sills, dikes, breccias, and tuffs that weather orange to brown (Mustard and Roots, 1997). Flows from member F are locally interstratified with the overlying glaciogenic deposits of the Rapitan Group–equivalent Eagle Creek formation (Mustard and Roots, 1997; Macdonald et al., 2010; Strauss et al., 2014b).

The Rapitan Group–equivalent Eagle Creek formation is locally in erosional contact with members A–E, and it interfingers with member F. A tuff near the base of the Eagle Creek formation yielded a U-Pb zircon age of 716.47 ± 0.24 Ma (CA-ID-TIMS; Macdonald et al., 2010). These glacial strata are locally overlain by various strata equivalent to the Cryogenian Hay Creek Group and the Ediacaran to Early Cambrian informal "Upper" group (Macdonald et al., 2011; Strauss et al., 2014b). The Bouvette Formation, a thick sequence of Cambrian to Devonian dolostone, regionally rests with angular unconformity on the Windermere Supergroup and older strata (Thompson et al., 1994; Mustard and Roots, 1997; Macdonald et al., 2011; Strauss et al., 2014b).

Synsedimentary tectonism during deposition of basal Windermere rocks has been investigated in the northern Canadian Cordillera (for example, Eisbacher, 1981, 1985; Jefferson and Parrish, 1989), in British Columbia (Root, 1987), and in the United States (Stewart, 1972;

Miller, 1985; Yonkee et al., 2014). In the Coal Creek inlier, for the Mount Harper Group, the oldest Neoproterozoic extensional structures in the area include the Trap Door and Early South Harper faults, both of which governed the depositional patterns of the Callison Lake and Seela Pass Formations (Fig. 2; Mustard, 1991; Mustard and Roots, 1997; Strauss et al., 2014b, 2015). The Mount Harper volcanics, Seela Pass Formation, and Callison Lake Formation occur north of the Early South Harper fault within the broad, informally termed Mount Harper synform (Fig. 2; Roots, 1987; Strauss et al., 2015). The Callison Lake synrift strata show evidence of thickening in the trough of the synform, which indicates that the folding was related to fault initiation at depth, with the development of growth stratigraphy above a fault tip (Schlische, 1995; Sharp et al., 2000). This type of hanging-wall synformal basin is well documented in extensional settings associated with normal fault systems (Schlische, 1995, 2003; Sharp et al., 2000; Gawthorpe and Leeder, 2000). The synform likely developed during the late stages of Callison Lake sedimentation and Mount Harper volcanism, as the broad synformal geometry is still apparent in the Mount Harper volcanics (Fig. 2C; Strauss et al., 2015). The synform plunges gently westward, preserving the younger volcanic members of the Mount Harper volcanics in the western Coal Creek inlier.

There are also a number of syn–Mount Harper volcanics brittle extensional structures. The north-side-down Tango Tarn fault was inferred from the distribution of members B and C of the Mount Harper volcanics and the Eagle Creek formation (Fig. 2; Roots, 1987; Mustard and Roots, 1997). The Early South Harper fault was also active during Mount Harper volcanics volcanism, but during most of the volcanic activity, the southern margin of the half graben remained high, as indicated by a transition from subaqueous hydroclastic breccia in the north to subaerial volcanism to the south (Roots, 1987). Following the eruption of the Mount Harper volcanics, the Early South Harper fault was reactivated as the partially reverse South Harper fault, and numerous SSE-striking faults and the North Harper fault were active (Fig. 2). The dominantly parallel SSE-striking faults do not cut the South Harper or North Harper faults, but they do cut the strata of the Rapitan Group–equivalent Eagle Creek formation (Fig. 2). The North Harper fault near the northern edge of the volcanics displays as much as 350 m of north-side-down displacement, indicated by the juxtaposition of the stratigraphically higher beds of the Eagle Creek formation and "Upper" group strata on the north side with the volcanics on the south side (Roots, 1987).
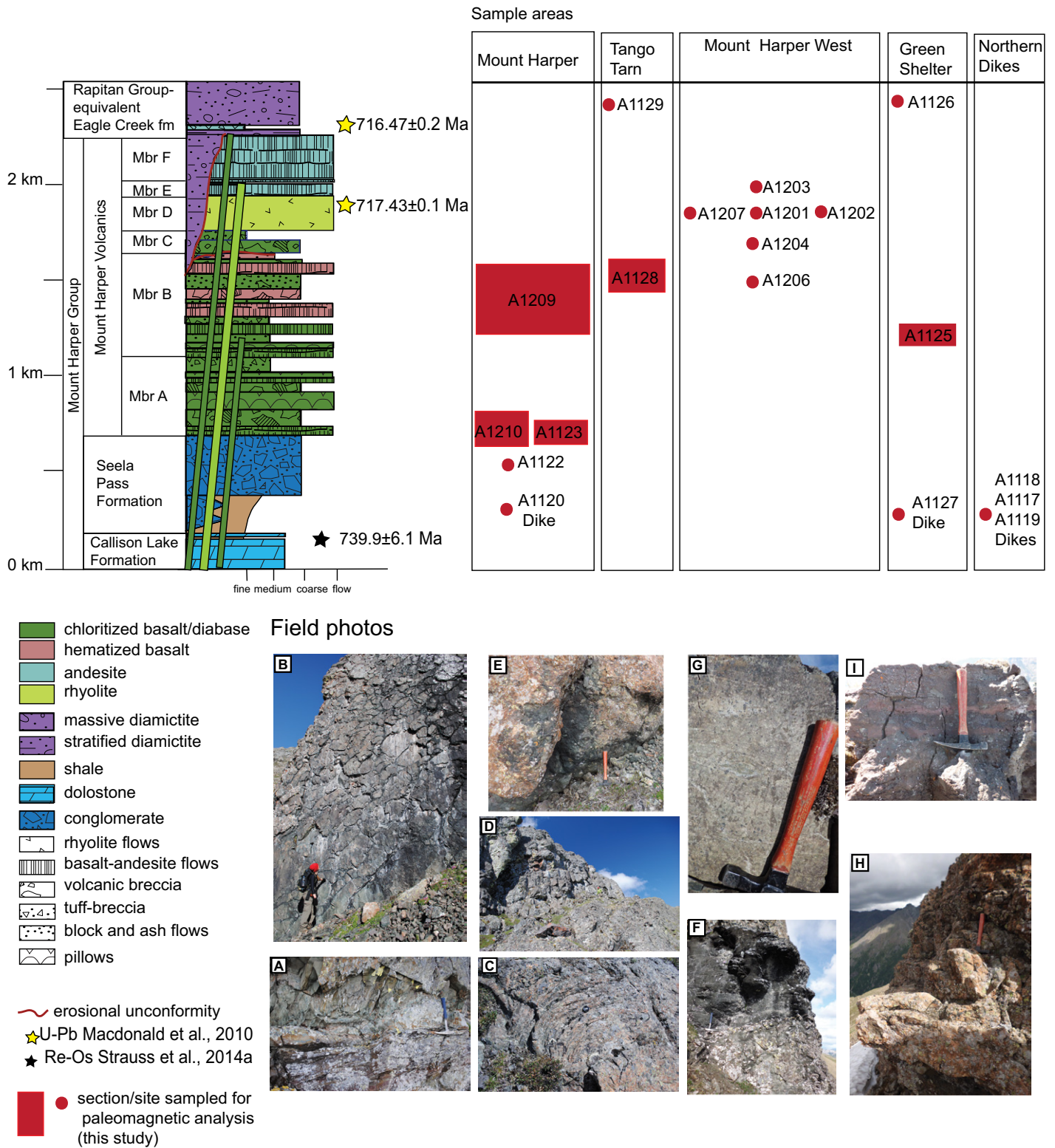
Figure 3. Composite stratigraphic section of the Mount Harper volcanics with the approximate stratigraphic position of sampled units along with field photos of the lower members (A and B) from Mount Harper and of the upper members (C, D, and E) from Mount Harper West (photos by J. Strauss and A. Eyster). (A) Contact between the Seela Pass Formation and member A. (B) Member A pillows. (C) Member B pahoehoe flow top. (D) Member B columnar joints. (E) Member C breccia. (F) Member C mafic tuff. (G) Member D flow banding. (H) Member E flows. (I) Basal Eagle Creek formation with volcanic clasts.

Observations of the regional outcrop extent of the Seela Pass Formation and Eagle Creek formation highlight the potential development of two distinct and slightly diachronous sub-basins with opposed but offset footwall scarps (Mustard, 1991). The emplacement of the Mount Harper volcanics may have been related to the development of an accommodation zone between the two offset grabens (Mustard, 1991; Mustard and Roots, 1997; Strauss et al., 2015). The angle between the SSE-striking faults and the North and South Harper faults could represent minor counterclockwise block rotations in a sinistral strike-slip system (Roots, 1987).

The modern expression of the Ogilvie Mountains is a result of late Mesozoic northward-directed shortening associated with the Cordilleran orogeny (Norris, 1997; Mair et al., 2006; Martel et al., 2011). Despite this regionally significant tectonic activity, map relationships in west-central Yukon suggest that the Coal Creek inlier acted as an orogenic welt, with wrench faults on the west side and counterclockwise faulting on the east side, but with minimal faulting or reactivation of faults observed within the inlier itself. In the Mount Harper volcanics, some primary structures in the area experienced minor reactivation, such as the Early South Harper fault (Roots, 1987).

Diagenetic Considerations

The Mount Harper volcanics experienced prehnite-pumpellyite-facies to lower-greenschist-facies metamorphism resulting from burial and fluid alteration during Mesozoic–Paleogene shortening associated with the Cordilleran orogeny (Roots, 1987; Greenwood et al., 1991; Mustard and Roots, 1997). The volcanics are highly hydrated and display abundant chlorite and sericite alteration (Cox et al., 2013). During alteration, volcanic glass was altered to quartz and feldspar, olivine phenocrysts were pseudomorphed into quartz and hematite, and plagioclase phenocrysts were replaced by clay minerals (Mustard and Roots, 1997). Primary paleomagnetic signals carried by magnetite can survive heating to the greenschist metamorphic range (300–500 °C) but not to the amphibolite range (600–750 °C; Pullaiah et al., 1975; Dunlop and Buchan, 1977). Furthermore, metamorphic changes that alter the ferromagnetic minerals can destroy the primary natural remanent magnetization and result in chemical remagnetization. Consequently, understanding the occurrence and nature of the magnetic minerals (hematite, magnetite, and titanomagnetite) is of particular interest for paleomagnetism studies. Alteration in members A and B involved hematite replacing olivine and albitization of

plagioclase that was later filled in with hematite. Primary iron oxidation likely occurred during the eruption of the hematized facies, in addition to later iron oxidation that occurred during secondary mobilization for both the chloritized and hematized volcanics. It is likely that syn-volcanic hematite formed in some of the sub-aerially erupted basalts (Mustard and Roots, 1997; Roots, 1987).

METHODS

Paleomagnetic samples were collected via drilling of small cores and hand sampling with orientations measured by a combination of Brunton and sun compass. The orientations of flow tops, along with any nearby sedimentary or water-lain units, were measured to correct for any tectonic tilting. Although the original volcanic units were likely tilted (gentle paleo-slopes), the areal and stratigraphic sampling was large enough to hopefully average any paleo-slope effects. The parallel orientation of flow banding and flow tops to sedimentary bedding suggests paleoslopes of less than 10°. Even so, errors in bedding corrections due to paleoslopes cannot be unambiguously quantified and may affect paleohorizontal corrections (Irving and Thorkelson, 1990).

We collected a total of 255 samples from 20 different rock units or localities, including two conglomerate tests and five measured sections. We sampled the upper and lower members of the Mount Harper volcanics, the Mount Harper volcanic dikes, and sedimentary deposits within the Seela Pass Formation and the Eagle Creek formation, with sampling concentrated at five main regions that ranged over 14 km across regional strike: Mount Harper, Mount Harper West, Tango Tarn, and Green shelter and Northern dikes (Figs. 2 and 3). The lower suite members were sampled at four of the regions, while the upper suite members were sampled only at Mount Harper West. At Tango Tarn and Green shelter, we collected both clasts and matrix samples for conglomerate tests from the base of the Eagle Creek formation. For the stratigraphic sections that spanned multiple flows/sites, we normally collected at least six samples total, with one to three samples per flow or stratigraphic horizon. We collected at least three samples from dikes ranging between ~2 and 12.5 m thick, focusing on sampling at the chilled margins, which are more likely to contain primary magnetization due to the smaller sizes expected for the magnetite carriers.

Individual samples were drilled and cut to specimens 2.5 cm in diameter and 2 cm long. One to two specimens were measured for each sample. Magnetization measurements were

made with a 2G Enterprises 755 superconducting rock magnetometer (SRM) in the Massachusetts Institute of Technology Paleomagnetism Laboratory using an automated sample handling system (Kirschvink et al., 2008). This instrument has a sensitivity of 10^{-9} Am^2 and is located in a magnetically shielded room (direct current [DC] field <150 nT). The natural remanent magnetism (NRM) was measured for all specimens. Then, we immersed a portion of the specimens in a liquid nitrogen bath to preferentially remove the magnetization carried by multidomain magnetite and hematite grains. This procedure was followed by alternating field (AF) demagnetization up to 15 mT on most of the specimens, and finally thermal demagnetization on all the specimens. The thermal demagnetization was conducted using an ASC Scientific thermal demagnetizer with peak DC fields inside <10 nT. Specimens were thermally demagnetized in steps of 2.5–50 °C until completely demagnetized. Similar demagnetization behaviors were observed in specimens that were subject to both thermal and AF demagnetization and those that were only thermally demagnetized.

Because lightning strikes can cause remagnetization, care was taken in the field to use both a sun compass and a Brunton compass to identify locations that may have experienced strong remagnetization. AF demagnetization up to 10–15 mT was able to remove randomly oriented minor secondary NRM components that may represent lightning-induced isothermal remanent magnetization (IRM) in 31 out of 220 specimens. A1128 was the only section from which specimens did not undergo AF demagnetization. However, specimens from A1128 did not demonstrate strong single-component magnetizations and high NRM intensities that would suggest lightning remagnetization. Lightning remagnetized specimens were identified in ~2% of analyzed specimens. Most of the specimens (~84%) from sites and measured sections yielded resolvable components of magnetization. Magnetic components were determined using principal component analysis of both best-fitting lines and, for 15% of the specimens, great circles (Kirschvink, 1980). When analyzing the data, we used a maximum angle of deviation (*MAD*) cutoff of 15° following the recommendation of Butler (1992), but in most cases the *MAD* angle was <10°. Specimen analysis was completed using the PaleoMag OS X program (Jones, 2002). If multiple specimens were prepared from a sample, then the specimen directions were averaged. In this and every other case, we applied Fisher statistics to calculate mean directions.

For our sites (single flows or cooling units), it was straightforward to calculate mean com-
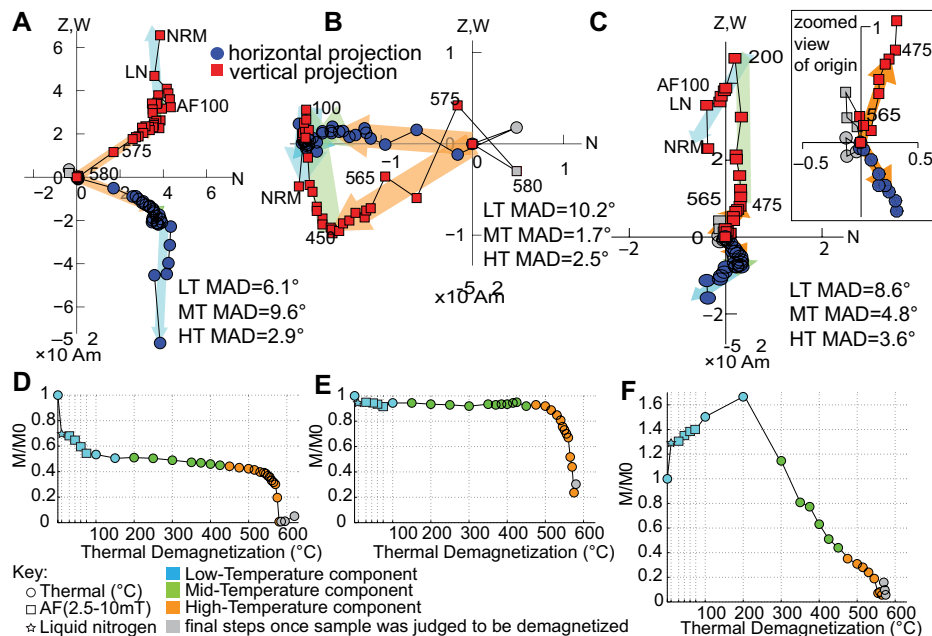
Figure 4. (A) Representative orthogonal projection diagrams showing the demagnetization of sample A1207-5 that carries HT1. (B) Representative orthogonal projection diagrams showing the demagnetization of sample A1203-3 that carries HT1. (C) Representative orthogonal projection diagrams showing the demagnetization of sample A1123-17 that carries HT2. (D–F) Corresponding $M/M0$ plots (M—magnetization and $M0$—initial magnetization). The stars represent the liquid nitrogen demagnetization step, the squares represent the alternating field (AF) demagnetization steps, and the circles represent thermal demagnetization. The representative orthogonal projections are shown using in situ coordinates. LT—low-temperature component; MT—mid-temperature component; HT—high-temperature component; MAD—maximum angular deviation; NRM—natural remanent magnetization. LN—liquid nitrogen.

ponent directions using all the samples from the site. For our sections, we typically had one to two samples for each flow and calculated mean component directions three different ways. In our first approach, we calculated section means using all the samples. For our second approach, we calculated section means, but using flow mean directions when possible. Here, when we collected multiple samples from a single flow, we calculated a mean flow direction. If this mean flow direction had $\alpha_{95} < 20°$ (for $n > 2$) or angular standard deviation $<20°$ (for $n = 2$), then it was combined with data from single sampled flows to obtain a section mean. In the third approach, we focused on directions from the individual flows within a section and only used data from flows with $n \geq 3$ and $\alpha_{95} < 20°$. We then calculated flow or site-mean component directions. The first two methods are more relevant to postemplacement magnetic acquisition (i.e., chemical remanent magnetization [CRM]), which is expected to cut across depositional flow boundaries, whereas the third method is most applicable to primary thermal remanent magnetization with eruptive events separated by brief hiatuses and non-negligible geomagnetic secular variation.

RESULTS

We classified the magnetizations based on their unblocking temperature range and directionality into a low-temperature (LT), a mid-temperature (MT), and two high-temperature (HT) component directions (Fig. 4). Although both conglomerate tests (A1126 and A1129) yielded random clast directions, only one of them yielded a coherent HT component matrix direction (A1126).

The three approaches that we used to calculate mean directions for the sections yielded essentially the same results (see supplementary Tables S2, S3, S4 and S5[1]). In the following discussions, we use our first approach, except when discussing HT1, where we also mention our results from the third approach (only using individual flows/sites) because we interpret that component to be a primary thermal remanence. The within-section/site precision parameters normally ranged between 10 and 50. The sections or sites that did not yield useful data

include those with $\alpha_{95} > 25°$ and two or fewer samples with resolvable directions (A1119, A1122, A1127), sites dominated by samples with no obvious decay to the origin that required great circle fits (A1118, A1201), and those with strong (moment $>10^{-6}$ A m^2) random directions that responded strongly to AF demagnetization and were interpreted to be the result of lightning (A1202, A1121). Additionally, two sites (A1117 and A1120) had three samples with resolvable directions and $\alpha_{95} > 20°$. The Tauxe and Watson (1994) fold test was applied, and uncertainty was quantified by utilizing bootstrapped data sets and repetition of the fold test for various percentages of unfolding.

The LT component direction was found in two sections (39 samples), representing members A and B (Figs. 5A and 5B). This component was removed during thermal demagnetization between 100 °C and 150 °C. The LT direction failed the Tauxe and Watson (1994) fold test. The maximum eigenvalue of the orientation matrices (τ_1) occurred at –10% unfolding, and the 95% confidence interval of bootstrapped samples is between –10% and 28% unfolding.

The MT component direction was found in eight sections encompassing 128 samples (Figs. 5C and 5D). These sites included member A, member B, member C, member E, and the Eagle Creek formation. This component was demagnetized upon heating to 425–500 °C. In 50% of the measured samples, this direction was tightly clustered ($\alpha_{95} < 10°$). The MT direction is also a post-tilting direction, as the maximum τ_1 occurred at –10% untilting, and the 95% confidence interval spans –10% to 8% unfolding.

Finally, the HT directions from the individual samples were observed to fall into two groupings, one with moderate positive inclinations toward the south and one with low negative inclinations toward the northeast. We label these the HT1 (Figs. 5E and 5F) and HT2 (Figs. 5G and 5H) components, respectively. Two sections (A1128 and A1209) yielded both HT1 and HT2 components with $\alpha_{95} < 20°$. Section A1128 was 191.5 m thick, and samples carrying HT1 were identified throughout the section, while samples carrying HT2 were scattered near the top of the section. Section A1209 was 273 m thick, and three samples carrying HT2 with
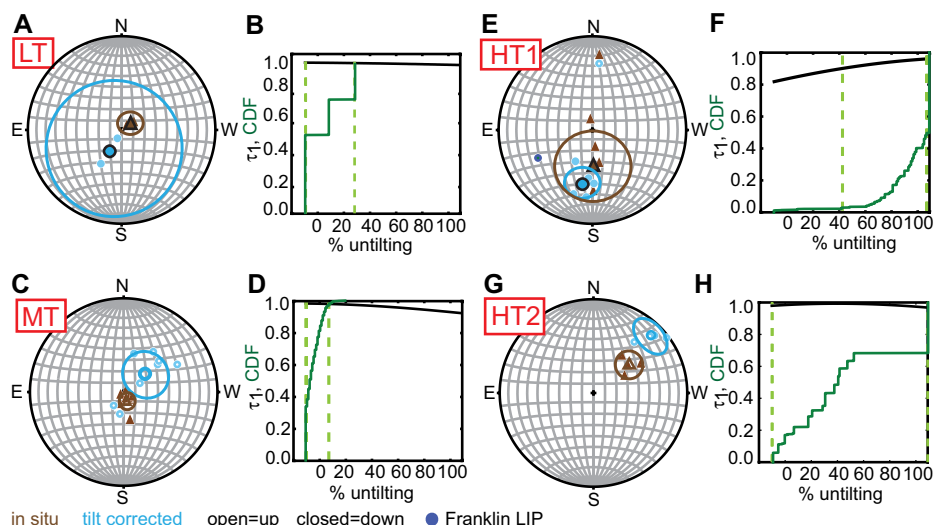
Figure 5. (A) Sections with a low-temperature (LT) direction. (B) Results from the Tauxe and Watson (1994) fold test. (C) Sections with a mid-temperature (MT) direction. (D) Results from the Tauxe and Watson (1994) fold test. (E) Section results for the first high-temperature (HT1) direction. Note that site A1207 has a high stability HT1 direction reversed from the rest. The direction expected from the Franklin large igneous province (LIP; Denyszyn et al., 2009a) is also indicated. (F) Results for HT1 from the Tauxe and Watson (1994) fold test. (G) Section results for the second high-temperature (HT2) direction. (H) Results for HT2 from the Tauxe and Watson (1994) fold test. For the plots of the section-mean directions, the in situ directions are indicated with brown triangles, and the tilt-corrected directions are indicated with blue circles, with negative directions represented by open symbols and positive directions represented by closed symbols. For the Tauxe and Watson (1994) fold tests, the black curves indicate maximum eigenvalue (τ_1) as a function of untilting. The green line is the cumulative distribution of the percent untilting required to maximize τ_1 for all the bootstrapped data sets. The dashed vertical lines are 95% confidence bounds on the percent untilting that yield the most clustered result (maximum τ_1). If the 95% confidence bounds include 0, then a pretilt magnetization is indicated. If the 95% confidence bounds include 100, then a post-tilt magnetization is indicated. If the 95% confidence bounds exclude both 0 and 100, syntilt magnetization is possible. CDF—cumulative distribution function.

The HT1 component passed the Tauxe and Watson (1994) fold test, as the maximum τ_1 occurred at 109% unfolding, with 95% confidence bounds from 42% to 109% unfolding, suggesting that the magnetization was acquired prior to folding. Using the third approach, the HT1 direction also passed the fold test, this time with maximum τ_1 at 92% unfolding, with confidence bounds from 89% to 109% unfolding.

One sampled unit (A1207, member D) displayed a reversed HT1 direction (Fig. 5E). This represents a double reversal, as this direction is reversed from those both stratigraphically above and below. In tilt-corrected coordinates, the reversal test (for the isolated reversed section) resulted in an observed angle between the mean direction of 16.8° and a critical angle of 38.7° calculated for the two sets of observations at which the null hypothesis of a common mean direction would be rejected with 95% confidence. However, due to the limited number of observations, the high value of the critical angle places the reversal test in the "indeterminate" classification of McFadden and McElhinny (1990). For the HT1 directions from the third approach, the observed angle is 18.0° and the critical angle is 18.7°; thus, these directions pass the reversal test with a C classification (McFadden and McElhinny, 1990). Finally, the primary nature of this direction is also supported by one of the conglomerate tests. An HT component was isolated in five clasts and four matrix samples from one of the conglomerate tests (A1126; see supplementary Fig. S1 [see footnote 1]). For the clasts, the critical value of the resultant vector (R_o) was 3.50 at the 95% confidence level, while the value of the resultant vector (R) was 2.2, which is less than the critical value and indicates that a uniform distribution can be rejected at the 95% confidence level (Watson, 1956). This contrasts with the four matrix samples with HT components that display the HT1 direction.

The HT2 direction was found in four sections (35 samples total) only from members A and B. The HT2 direction was more likely to be isolated using great circle fits in the principal component analysis than the HT1 direction. Depending on the sample, the HT2 component could be removed after heating to 350–680 °C, but in most samples, it was removed by heating up to 570 °C or 680 °C. These unblocking temperatures are consistent with the temperatures expected from magnetite and hematite. The Tauxe and Watson (1994) fold test for the HT2 direction was ambiguous, with the maximum τ_1 occurring at 40% untilting, but with the 95% confidence interval spanning –10% to 109% unfolding.

unblocking temperatures expected for hematite were collected from near the top, as well as one sample near the base. Additionally, one sample carrying HT1 was analyzed from the top of A1210. In most cases where we collected multiple samples from a single flow, HT1 and HT2 were found in different flows. However, in section A1128, one flow had one sample with HT2 (A1128–50), while the other samples from that flow carried HT1. In two cases, a sample displayed both HT1 and HT2 directions: Both specimens from sample A1209–17 displayed a HT1 component direction unblocked by 575 °C and HT2 unblocked at 680 °C, and sample A1209–4 displayed a HT1 direction unblocked at 565 °C and a higher-temperature circle fit to HT2.

In total, using the first approach, we resolved HT1 site/section mean directions with $\alpha_{95} < 20°$ in one site and four sections (60 samples), including members B, D, and E, along with the

matrix from the Rapitan Group–equivalent strata of the Eagle Creek formation. Using the third approach, we identified HT1 site mean directions with $\alpha_{95} < 20°$ in seven flows/sites (34 samples) from members B, D, and E. In most samples, this component was fully demagnetized between 565 °C and 575 °C, indicating magnetite as the principal ferromagnetic carrier. Among all the samples, some were demagnetized much earlier than 565 °C, starting at 400 °C. There were four samples where the HT1 direction had unblocking temperatures between 605 °C and 680 °C. Under further examination, it was observed that these samples, carrying a HT1 with high unblocking temperatures, also displayed a substantial decay of the intensity of the magnetization at 580 °C in the direction of HT1. From this, we conclude that the HT1 direction is carried by both magnetite and hematite in these samples.

MAGNETIC CARRIERS FOR HT COMPONENT DIRECTIONS

Thin sections were made from select samples that carried the HT1 (A1203, A1207) and HT2 (A1128, A1210) component directions. The samples carrying the HT1 component were observed to include small interlocking opaque minerals, likely magnetite and titanomagnetite, in the matrix. The vesicles in these samples tended to be filled with calcite. The samples that displayed the HT2 direction were found to have some smaller opaque minerals in the matrix, with some larger likely magnetite crystals, as well as vesicles filled with quartz and titanomagnetite. Finally, we observed some fine hematite staining that preferentially filled cracks and veins. Because multidomain (MD) grains visible in the microscope do not necessarily carry the bulk of the stable magnetization (Jackson, 1990), we relied on rock magnetism experiments to characterize the bulk properties of the magnetic carriers. The magnetic mineralogy of 16 different samples was analyzed with IRM acquisition and IRM backfield experiments, thermal demagnetization of saturation IRM (sIRM), AF demagnetization of sIRM, and hysteresis experiments. We applied stepwise IRM acquisition in a field up to 2.5 T to determine the coercivity spectra and saturation fields and thereby resolve distinct populations of ferromagnetic minerals. Following the IRM acquisition, backfield IRM was applied in order to determine the coercivity of remanence (H_{cr}). We obtained hysteresis experiments with maximum fields of 1 T using the vibrating sample magnetometer (VSM) in the Massachusetts Institute of Technology laboratory of C. Ross to determine the values of saturation magnetization (M_s), saturation remanence (M_{rs}), and coercivity (H_c). We used these parameters to constrain the domain states of the magnetic carriers. Next, for five samples carrying the HT1 component and five samples carrying the HT2 component, we investigated the thermal demagnetization of sIRM to identify the magnetic carriers based on their unblocking behavior. Finally, on six samples carrying the HT1 component and four carrying the HT2 component, we conducted AF demagnetization of the sIRM to determine the crossover values and the strength of the interactions between the ferromagnetic grains (Cisowski, 1981).

Rock Magnetism Results

IRM Acquisition and Backfield IRM Experiments

Following Kruiver et al. (2001), we display the IRM acquisition data on a linear acquisition plot (LAP) and a gradient of acquisition plot (GAP; Fig. 6). We decomposed the measured IRM data into cumulative log-Gaussian (CLG) curves, each of which is characterized by the sIRM, mean coercivity ($H_{1/2}$), and dispersion (dp). $H_{1/2}$ is a measure of the coercivity of remanence H_{cr} if a sample contains only a single population of ferromagnetic grains. The two most important magnetic phases in geological materials are magnetite and hematite, which have maximum coercivities of ~300 and >1000 mT, respectively (O'Reilly, 1984; Banerjee, 1971). The principal ferromagnetic phase in samples that carried origin-trending HT1 reached saturation magnetization before 300 mT, consistent with a lower-coercivity mineral such as magnetite (Figs. 6A and 6B). Furthermore, samples carrying an HT1 direction displayed a single peak in the GAP plots, suggesting that they contained only one significant ferromagnetic mineral (Figs. 6A and 6B). The dike samples (A1120-4 and A1120-3) contained a minor component of a higher-coercivity mineral, possibly hematite or pyrrhotite, but the peak on the GAP plot was difficult to distinguish. These samples reached 99.5% of their sIRM at 550–840 mT. For all samples carrying the HT1 component, the backfield IRM experiments indicated H_{cr} values of 26–47 mT, consistent with a low-coercivity magnetic mineralogy.

All samples with an HT2 component reached 99.5% of the sIRM between 500 mT and 2000–2400 mT (Figs. 6A and 6B), which suggests these samples contain a high-coercivity mineral such as hematite. In addition, most of the samples that carried the HT2 direction displayed two peaks, suggesting two populations of magnetic carriers (Figs. 6A and 6B), with the higher-coercivity component containing 75% of the sIRM. Of the HT2 component–bearing samples, sample A1123-10 displayed only one dominant peak, with 99.5% of the saturation reached at 500 mT. This suggests that in rare cases, a lower-coercivity mineral, such as low-coercivity magnetite, carries the HT2 direction. The backfield IRM experiments generally indicated H_{cr} of 220–490 mT, which is higher than those of samples carrying HT1, except for that of A1123-10, which had an H_{cr} of 31 mT.

Hysteresis Experiments

We obtained hysteresis parameters after processing the uncorrected hysteresis data by closing the ascending and descending loops when needed, subtracting the high field slope, and adjusting such that the *y* intercepts were equal (plots and analysis were done using the PmagPy cookbook code; methods discussed in Tauxe et al., 2010). The uncorrected data for all samples displayed loops with strong positive (paramagnetic) high field slopes and potbellied shape. This paramagnetic component dominates the uncorrected data for most samples (dashed lines in the hysteresis curves in Fig. 6A), except for four samples that had an uncorrected shape closer to pseudo-single-domain shape: A1210-23 (carrying HT1), A1123-5, A1123-10, and A1123-17 (all carrying HT2). Potbellied behavior can result when the magnetic carriers

Figure 6 (*on following page*). **Results of rock magnetic experiments. (A) Comparison of rock magnetic results for representative samples shown in Figure 3 carrying the first and second high-temperature components (HT1 and HT2). Sample A1207-5 from member D carries reversed HT1, and sample A1203-3 from member E carries normal HT1, while sample A1123-17 from member A carries HT2. (i) Linear acquisition plot. (ii) Gradient curve of isothermal remanent magnetization (IRM) acquisition. (iii) Backfield IRM data. (iv) Thermal demagnetization of saturation IRM (sIRM). (v) Alternating field (AF) demagnetization of sIRM. (vi) Hysteresis curves for A1207-5 carrying HT1, where dashed line is raw data, and solid line indicates data corrected for paramagnetic slope. (vii) Hysteresis curves for A1203-3 carrying HT1, where dashed line is raw data, and solid line indicates data corrected for paramagnetic slope. (viii) Hysteresis curves for A1123-17, where dashed line is raw data, and solid line indicates data corrected for paramagnetic slope. (B) Comprehensive plot of all rock magnetic results for selected samples carrying HT1 (left side) and HT2 (right side). (i, ii) Linear acquisition plots. (iii, iv) Gradient curves of IRM acquisition. (v, vi) Backfield IRM data. (vii, viii) Thermal demagnetization of sIRM. (ix, x) AF demagnetization of sIRM. (C) Day plot of results from hysteresis experiments. Blue asterisks mark results for samples carrying HT1, while red circles mark those for samples carrying HT2. Also shown are boxes marking single-domain (SD), pseudo-single-domain (PSD), multidomain (MD), and superparamagnetic (SP) regimes as well as the MD-SD mixing curve of Dunlop (2002) in green. Inset shows behavior of samples carrying HT2, specifically, the wasp-waisted behavior of A1123-17, likely due to dual-population ferromagnetic mineralogy and the SD hematite behavior of A1209-18. H—applied field intensity, M—magnetization, H_{cr}—coercivity of remanence, H_c—coercivity, M_s—saturation magnetization, M_{rs}—saturation remanence.**
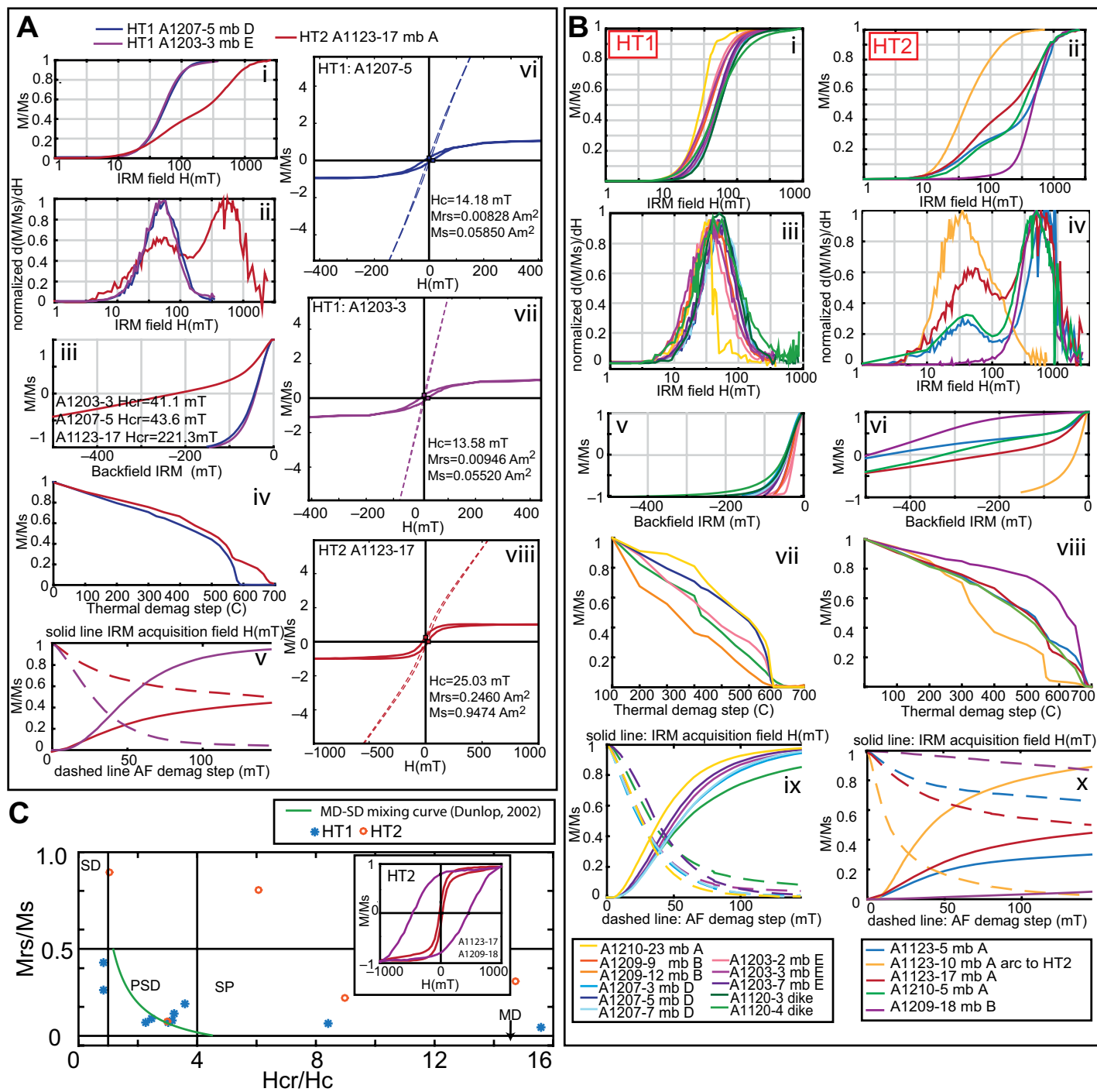
Figure 6.

are a mixture of single-domain (SD) and fine-grained superparamagnetic (SP) magnetite. For samples carrying HT1, the shapes of the corrected hysteresis curves were consistent with those expected for pseudo-single-domain grains reaching M_s by ~300 mT (Fig. 6A, right side).

As most samples carrying HT2 were not fully saturated by the maximum field allowed by the VSM, minor hysteresis loops were obtained.

The corrected hysteresis curves displayed pseudo-single-domain behavior (A1123-10), wasp-waisted (A1123-5, A1123-17, A1210-5), and single-domain hematite behavior (A1209-18). The wasp-waisted curves occurred when there were multiple fractions of magnetic minerals with strongly contrasting coercivity or in the presence of a significant superparamagnetic component. As already determined from the

IRM acquisition experiments, many of the samples carrying HT2 had two populations of ferromagnetic carriers with distinct coercivity ranges.

Saturation magnetization, saturation remanence and coercivity, as well as backfield coercivity, were used to construct a Day plot to determine if the magnetic carriers were SD, MD, pseudo-single-domain (PSD), or SP (Fig. 6C). Samples carrying the HT1 component were

either in the PSD range or a mixture of SD and MD particles, but there was no real trend in the data along any MD-SD mixing lines. Additionally, some samples carrying the HT1 component were located far to the right, likely indicative of SP-SD mixtures of magnetite grains (Dunlop, 2002). Day plots are not as informative for samples with multiple magnetic minerals, and when considering the samples carrying HT2 and there is no dominant clustering observed.

Thermal Demagnetization of sIRM

The thermal demagnetization of sIRM of samples carrying HT1 displayed a distributed range of unblocking temperatures (T_{ub}) up to 580 °C, in some cases with ~70% of the remanence destroyed, followed by a steep drop at 580 °C, as expected for magnetite. These data combined with the IRM acquisition curves suggest that HT1 is carried by low-coercivity magnetite. In one sample from a dike (A1120-4), there was a minor decay at 100–325 °C, followed by a gradual decay to 650 °C, indicating a small contribution of pyrrhotite or Ti-rich titanomagnetites as well as hematite. Some magnetization carried by hematite or pyrrhotite is also suggested based on a higher-coercivity component in the IRM acquisition curves.

Samples carrying the HT2 direction were observed to have only hematite or both hematite and magnetite as magnetic carriers. We observed a distributed range in unblocking temperatures for the samples with both hematite and magnetite, with steeper drops observed at 560 °C, 580 °C, and 680 °C. Sample A1123-10, which carried a great circle fit toward HT2, displayed a drop at both 560 °C as well as at 680 °C, consistent with the presence of titanomagnetite and hematite.

AF Demagnetization of sIRM

For samples carrying the HT1 component, AF demagnetization of sIRM resulted in median destructive fields (MDF) of ~25–35 mT, which are typical for PSD magnetite. The field at which the demagnetization and acquisition curves cross (the crossover point Rx) is sensitive to particle interaction. All the crossover points for HT1 occurred at normalized M_s values <0.5 (between 0.3 and 0.4), suggesting a moderate degree of interparticle interaction. The shape of the AF demagnetization curves is softer than expected for noninteracting SD grains. Additionally, one of the dikes (A1120-4) was not fully demagnetized by 145 mT (the highest AF level available), suggesting the presence of a high-coercivity mineral such as pyrrhotite, hematite, or goethite. As seen in Figure 6B, most samples carrying HT2 were not fully demagnetized by 145 mT, which was the AF demagnetization capability of the instrument. Most curves therefore went off the scale, and thus a crossover point was not determined. One sample, A1123-10, had an MDF of 15 mT, with low MDF more consistent with a MD-dominant sample, and a crossover point at $M/M_s = 0.3074$, suggesting the presence of negatively interacting SD minerals or MD minerals.

We conclude that the magnetic mineralogy of samples carrying HT1 can be characterized by a single low-coercivity population of interacting magnetite that is likely PSD or a mixture of SD and SP states. The magnetic mineralogy of most samples carrying HT2 includes two populations of minerals with distinct ranges of coercivities. Observed unblocking temperatures suggest that the higher-coercivity mineral is hematite, and the lower-coercivity mineral is magnetite. In some cases, the samples carrying HT2 only have high-coercivity SD hematite as the magnetic carrier.

DISCUSSION

Timing of Magnetizations Determined by Fold Tests

As discussed already, while the LT and MT directions are characterized by failed fold tests and the HT2 direction results in an ambiguous fold test, the HT1 direction passes this important confidence criterion. For the HT1 fold test, the most important sections were those of members A and B with dips to the SW near Tango Tarn and Mount Harper, and members D and E with shallow dips to the north near Mount Harper West (Fig. 2C). The difference in paleohorizontal orientation between these areas is likely related to the synvolcanic Mount Harper synform, which initially developed during extensional activity on the Mount Harper fault and deposition of the Callison Lake Formation. As HT1 passes the fold test, it was likely acquired before the folding involved in the Mount Harper synform and therefore may represent a primary magnetization. It may be confusing that the Mount Harper volcanics are characterized by a remanence that predates folding while at the same time the folding was syneruptive; however, because the volcanics were likely erupting at the same time as the synform was developing, the primary magnetization was acquired on much shorter time scales (related to the cooling of the lavas), while the synform developed over a longer time scale—this difference in the timing results in passage of the fold test and a prefolding primary magnetization. For all of the flows, the magnetization was acquired before it was folded or tilted, and thus the most clustered result for the HT1 direction is when all flows were at around 100% of the untilting, i.e., restored close to paleohorizontal.

The failure of the LT direction fold test suggests that the LT direction postdates any activity on the North Harper fault, which displaces the Bouvette Formation. The failure of the MT fold test suggests that it was likely acquired after the development of the Mount Harper synform and movement on the SSE-striking faults. As the HT2 fold test is ambiguous, it is difficult to interpret the timing of the HT2 overprint.

Discussion of the Primary Nature of HT1

Several lines of evidence suggest that the HT1 direction is primary. The HT1 direction passes a fold test defined by the Mount Harper synform and passes a conglomerate test. Also, the presence of a reversed unit adds weight to the conclusion that HT1 is primary. The rock magnetism experiments suggest that HT1 is carried by a single low-coercivity population of interacting magnetite grains that are likely PSD or a mixture of SD and SP, which is consistent with the expected primary ferromagnetic mineralogy of volcanic rocks. In the few cases where HT1 was carried by hematite, there is evidence that the basalt flows erupted subaerially, and we suggest that this caused some early alteration and hematization, resulting in a practically primary magnetization but carried by hematite.

With respect to secular variation, based on the geochronological constraints, the Mount Harper volcanics erupted between ca. 739 and 716 Ma (Macdonald et al., 2010; Strauss et al., 2014a), but the eruption duration was likely much shorter than that. Typically, around five lava flows are used to characterize paleosecular variations at a site (McElhinny and McFadden, 1997; Johnson and Constable, 1995). Here, our stratigraphic sections vary in thickness, but section A1128 spans around 200 m and has multiple flows with samples carrying the HT1 direction throughout. The time interval represented by a thick section, such as this, is likely >1 m.y. and long enough to average out secular variations (McElhinny and Merrill, 1975).

Butler (1992) suggested using the scatter of virtual geomagnetic poles (VGPs) to determine whether secular variation has been averaged out or if there is excess scatter in the data. If secular variation has been adequately sampled, the observed angular dispersion of site-mean VGPs should be consistent with that predicted for the paleolatitude of the sampling sites. Assuming that the last 0–5 m.y. recorded similar field behavior to that in the Neoproterozoic, the observed angular dispersion for 15–38° paleolatitude should be around 12.1°–16.46° (Table 4 of McElhinny and McFadden, 1997). For our site/flow mean VGPs determined from approach three, the observed angular dispersion is

7.3°, i.e., less than the expected dispersion, suggesting that we may not have successfully averaged out secular variation. However, another method for investigating secular variation is to use confidence envelopes for A_{95} as a measure of secular variation (Deenen et al., 2011). Deenen et al. (2011) investigated values of A_{95}, given N, the number of paleomagnetic sites, and K, the dispersion. Comparing our VGP data ($K = 71.8$, $N = 7$, $A_{95} = 7.2°$) to the A_{95} envelopes of Figure 3 of Deenen et al. (2011), our data fall in the gray envelope, which indicates that the observed scatter is consistent with adequately averaging secular variation.

Our HT1 pole passes six out of the seven reliability criteria of Van der Voo (1990), failing the structural control and tectonic coherence criterion. Specifically, the primary nature of this direction is supported by a well-determined rock age and sufficient documentation in one site and four sections (approach 1: 1 site and 4 sections, 60 samples, $\alpha_{95} = 14.3°$, $A_{95} = 13.8°$, both <16°, and $k = 29.5$ and $K = 31.6$, both >10; approach 3: 7 sites, 34 samples $\alpha_{95} = 7.7°$, $A_{95} = 7.2°$, both <16°, and $k = 61.8$ and $K = 71.6$, both >10). Additionally, we applied adequate demagnetization with vector subtraction and benefit from a positive fold test, a positive conglomerate test, presence of reversals, and no resemblance to younger paleopoles.

When considering the key pole criteria of Buchan (2014), HT1 is related to a robust age, the primary remanence is properly isolated, and secular variation may have been averaged out. With regard to the Buchan (2014) field tests that constrain the magnetism to be primary, our fold test just establishes the relative timing of the magnetization. Although our conglomerate test is on the younger sediments of the Eagle Creek formation, the matrix in that conglomerate does carry HT1, so that indicates that the test itself still constrains the magnetization as an intraformational (Mount Harper volcanics combined with Eagle Creek formation) conglomerate test on HT1.

Interpretations of Directions and Comparison to the Laurentian Apparent Polar Wander Path

Four paleomagnetic poles were distinguished in this study: a low-temperature (LT), mid-temperature (MT), and two high-temperature poles (HT1-primary and HT2-chemical overprint; Table 1). These poles are plotted in Figure 7 along with the Laurentian apparent polar wander path (APWP) from 510 Ma to the present (Torsvik et al., 2012), for 200 Ma to the present (Besse and Courtillot, 2002), and for 230–50 Ma (Kent and Irving, 2010), along with a schematic pole envelope that encompasses Cryogenian–Ediacaran poles from Laurentia (Park, 1995, 1997; Mitchell et al., 2011, and references therein), and the pole for the coeval Franklin LIP (Table 1). For the Franklin LIP pole, we used the autochthon-only mean pole (D+09can) from Denyszyn et al. (2009a), which overlaps with the older mean pole of Buchan et al. (2000).

This primary pole (HT1) is located at similar longitudes as the Mount Harper pole interpreted to be primary by Park et al. (1992), but the errors associated with the pole have been improved, and the latitude has been refined. Our paleomagnetic data from the coeval Neoproterozoic Mount Harper volcanics (HT1, this study) and Franklin LIP (Denyszyn et al., 2009a) are differ-ent: The HT1 pole longitude is ~50° east of what is expected based on the Franklin pole (Fig. 7A). There are at least three options for explaining this difference: (1) secular variation of the geomagnetic field, specifically a 50° excursion during the eruption of the Mount Harper volcanics; (2) rapid oscillatory motion of Laurentia, which could have been due to either plate motion or true polar wander (TPW); or (3) a counterclockwise tectonic block rotation relative to Laurentia subsequent to the eruption and emplacement of the Mount Harper volcanics.

Anomalous directions dissimilar from the Franklin pole were previously recovered from Borden dikes on Baffin Island (Christie and Fahrig, 1983; Pehrsson and Buchan, 1999), and dikes on Ellesmere and Devon Islands (Denyszyn et al., 2009a, 2009b), as well as from the Rapitan Group in the Mackenzie Mountains (Park, 1997; Morris, 1977). Initially, the northwest-trending Borden dikes were thought to be part of a much older event, due to an older ca. 950 Ma age, crosscutting relationships, and a steep paleomagnetic direction (Christie and Fahrig, 1983). Reevaluation of these dikes by Pehrsson and Buchan (1999) updated the age to Franklin times (ca. 720 Ma) and suggested that the steep magnetizations resulted from the superposition of a Cretaceous–Tertiary–aged CRM on normal and reversed primary Franklin components. The anomalous paleomagnetic results from the Franklin-affiliated dikes on Ellesmere and Devon Islands were shown to be due to chemical remagnetization (Denyszyn et al., 2009b). In contrast, at Mount Harper, we have documented a double reversal, presence of the HT1 direction throughout the Mount Harper volcanic complex, and a robust single-domain

TABLE 1. PALEOMAGNETIC DIRECTIONS AND POLES

| Component | In situ directions | | | | Tilt-corrected directions | | | | Paleomagnetic poles[†] | | | | MHV paleolatitude |
	Declination/ inclination (°)	k	$N*$	α_{95} (°)	Declination/ inclination (°)	k	$N*$	α_{95} (°)	Latitude/longitude (°N/°E)	A_{95} (°)	N	K	(°)
LT	54.0/80.9	1886.5	2	5.8	209.2/69.7	21.6	2	56.6	69.6/265[§]	10.8	2	533.83	NA[##]
MT	161.7/–82.1	89.6	8	5.9	49.1/–65.4	9.5	8	20.1	77.7/197.4[§]	10.4	8	29.4	NA[***]
HT2	52.2/–50.3	62.3	4	11.7	45.8/–15.3	39.0	4	14.9	14.5/176.0[§]	13.4	4	49.8	NA[***]
									–9.8/174.3[#]	9.8	4	88.1	NA[***]
HT1 approach 1	179.1/58.1	6.9	5	31.3	190.0/42.1	29.5	5	14.3	0.4/210.7[#]	13.8	5	31.6	24.3
HT1 approach 3	174.9/48.3	18.1	7	14.6	182.4/44.4	61.8	7	7.7	1.4/218.1[#]	7.2	7	71.6	26.1
70 Ma[**]	NA[***]	NA[***]	NA[***]	NA[***]	NA[***]	NA[***]	NA[***]	NA[***]	75.9/204.7	4.6	7	169.8	NA[***]
77.9 Ma[††]	NA[***]	NA[***]	NA[***]	NA[***]	NA[***]	NA[***]	NA[***]	NA[***]	74.7/207.4	5.9	14	47.2	NA[***]
80 Ma[§§]	NA[***]	NA[***]	NA[***]	NA[***]	NA[***]	NA[***]	NA[***]	NA[***]	74.5/201.3	7.9	7	ND[†††]	NA[***]
Franklin LIP[##]	NA[***]	NA[***]	NA[***]	NA[***]	243.2/35.0	NA[***]	NA[***]	NA[***]	6.7/162.1	3.00	26	ND[†††]	19.3

*N—number of sites and/or sections.
[†]Poles calculated as means from site/section poles for the Mount Harper volcanics (MHV; 64.7°N, 139.9°W) with HT1 directions from site A1207 reversed and only the matrix HT1 directions from site A1126.
[§]Calculated from the in situ direction.
[#]Calculated from the tilt-corrected direction.
[**]Pole from Kent and Irving (2010).
[††]Pole from Besse and Courtillot (2002).
[§§]Pole from Torsvik et al. (2012).
[##]D+09can pole from Denyszyn et al. (2009a).
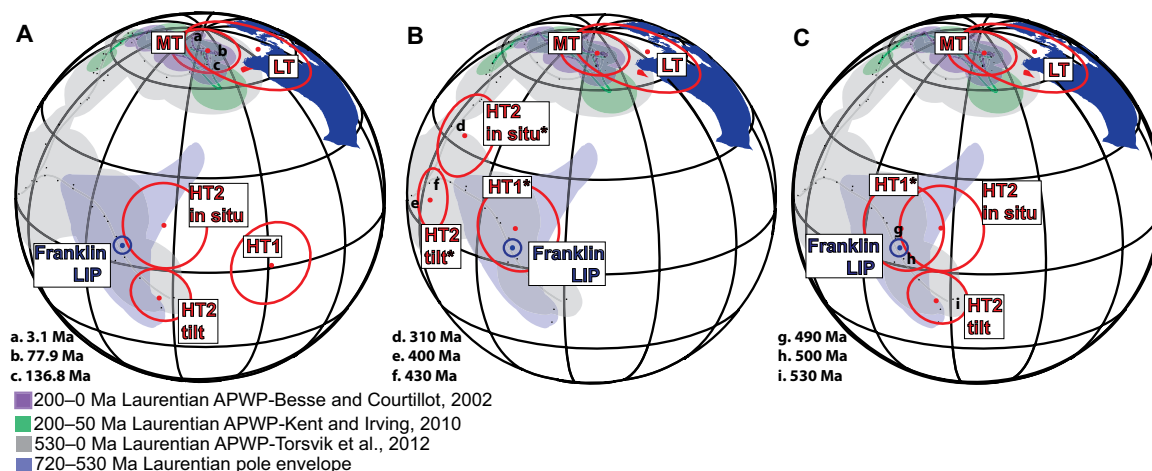[***]NA—not applicable.
[†††]ND—no data.

Figure 7. Paleomagnetic poles from this study (red, with the circle identifying the circle of A_{95} confidence). Blue indicates the Franklin large igneous province (LIP) pole, i.e., the D+90can pole of Denyszyn et al. (2009a), with the circle identifying the circle of A_{95} confidence. The 200 Ma to present apparent polar wander path (APWP) is from Besse and Courtillot (2002), the 230–50 Ma APWP is from Kent and Irving (2010), the 530 Ma to present Laurentian APWP is from Torsvik et al. (2012), and the 720–530 Ma Laurentian pole envelope is from data of Park (1995, 1997) and compiled by Mitchell et al. (2011). (A) Poles in current positions. (B) Poles plotted with expected locations if the rotation occurred between the Carboniferous and Cretaceous, after the second high-temperature component (HT2) overprint was acquired but before the mid-temperature component (MT) and low-temperature component (LT) overprints. (C) Poles plotted with expected location if the rotation occurred in the Cryogenian–Ediacaran, before the HT2, MT, and LT overprints were acquired. The asterisks indicate a pole in a restored (prerotation) position, and the lowercase letters indicate poles of particular times of interest (a, b, c from APWP of Besse and Courtillot, 2002; d, e, f, g, h, i from APWP of Torsvik et al., 2012). HT1—first high-temperature component.

magnetite carrier, all suggestive of a primary magnetization. Moreover, calculation of the secular variation captured in the stratigraphic sections suggests that we have adequately sampled for secular variation.

Rapid TPW could involve up to 90° rotation of the crust and mantle relative to the spin axis due to changes in Earth's moment of inertia (e.g., Kirschvink et al., 1997). As paleomagnetic studies assume plate-tectonic speeds have remained relatively constant through time, observations of large, rapid (>20 cm/yr) continental movements, particularly in the Neoproterozoic, have been attributed instead to TPW (Kirschvink et al., 1997; Li et al., 2004; Maloof et al., 2006). For example, it has been suggested that a rising superplume centered under Rodinia initiated a Neoproterozoic TPW event (800–750 Ma) as well as the breakup of Rodinia (Li et al., 2004). As noted already, the Mount Harper volcanics were emplaced coeval with the Franklin LIP, and no regular trend in the paleomagnetic data was observed stratigraphically through the Mount Harper volcanics members. These observations suggest that it is unlikely that the rotation was caused by rapid TPW, and thus we consider the third possibility: that the rotation was due to a counterclockwise tectonic block rotation subsequent to the eruption and emplacement of the

Mount Harper volcanics and the Franklin LIP. The HT1 pole can be restored to its original position aligned with the Franklin LIP by rotating the Mount Harper volcanics ~50° clockwise (Figs. 7B and 7C).

As for the HT2 direction, rock magnetic results and unblocking temperatures suggest that hematite is its main magnetic carrier. As high temperatures were needed to thermally demagnetize this component (680 °C for many samples), this requires a very high metamorphic temperature in order to have a thermoviscous origin; therefore, we interpret this result as being a CRM. CRM is acquired as a magnetic mineral nucleates and grows through a critical volume at which its magnetic direction becomes stable with respect to thermal fluctuations (Stokking and Tauxe, 1990). This can occur during mineral alteration (e.g., oxidation of magnetite to hematite) or mineral precipitation (grain growth or crystallization), which may accompany weathering, diagenesis, or low-grade metamorphism (Stokking and Tauxe, 1990). CRM remagnetization overprints via secondary precipitation/growth of hematite or conversion to hematite are generally a result of large-scale fluid flow during orogenesis (Miller and Kent, 1988), pronounced hydrothermal events (Witte and Kent, 1991), hydrothermal systems circulating in permeable

rocks below basalts (Wynne et al., 1998), or migration of fluids along fractures and unconformities during uplift-enhanced surface meteoric fluid circulation (Geissman and Harlan, 2002; Preeden et al., 2009).

As the HT2 direction resulted in an ambiguous fold test, both the in situ and tilt-corrected poles are plotted (Fig. 7). The HT2 pole overlaps with other Laurentian paleomagnetic poles in both prerotation and postrotation positions (Figs. 7B and 7C). If the rotation occurred after HT2 was acquired (Fig. 7B), then after restoring the HT1 pole to align with the Franklin pole, the HT2 direction is similar to the Carboniferous (HT2 in situ) and Silurian–Devonian poles (HT2 tilt) of the Laurentian APWP (Torsvik et al., 2012). Alternatively, if the rotation occurred before HT2 was acquired (Fig. 7C), the HT2 pole is similar to the Cryogenian to Ediacaran poles and later 500–490 Ma poles (HT2 in situ) and 530–500 Ma poles (HT2 tilt). At intermediate restoration times, the HT2 in situ pole bears similarity to Laurentian Cambrian–Ordovician poles.

Throughout the northern Cordillera, there have been several periods of orogenic, hydrothermal, and igneous activity that could have induced hematization that facilitated the acquisition of the HT2 overprint. These events could

include Ordovician–Mississippian mineralization events that resulted in localized sedimentary exhalative deposits (SedEx) or volcanogenic massive sulfide (VMS) deposits (the Late Devonian thermal event, the Howard's Pass deposits, Tom and Jason deposits), as well as Cambrian–Late Ordovician Selwyn basin volcanism and Neoproterozoic hematization events (e.g., Morrow et al., 1990; Goodfellow et al., 1995; Park, 1997; Martel et al., 2011; Ootes et al., 2013; and references therein). Of these, the Neoproterozoic hematization events have produced documented paleomagnetic overprints (Park, 1997), while the effect of the other events on paleomagnetic data is currently unclear. Thus, the most straightforward explanation is that the HT2 direction is Neoproterozoic to early Paleozoic in age and postdates the rotation.

The MT direction unblocks around 450 °C, and given the usual temperatures for greenschist-facies metamorphism, this direction is likely a thermo-viscous remanent magnetization (TVRM) due to regional metamorphism associated with the Cordilleran orogeny. In the Yukon, this metamorphism is broadly constrained to be Late Jurassic to Cretaceous in age, with widespread mid-Cretaceous metamorphism along with intrusions of granitic rocks (Greenwood et al., 1991; McMechan et al., 1992; Tempelman-Kluit, 1970; Murphy, 1997). In the Ogilvie Mountains and Selwyn basin, the youngest deformed strata observed are dominantly Late Cretaceous, and intrusions of the mid-Cretaceous Selwyn plutonic suites are large with minimal postemplacement deformation (Yorath, 1992; McMechan et al., 1992). However, deformation did continue later, as suggested by folded Paleocene–Eocene stratigraphy in the northern Ogilvie and Wernecke Mountains. When considering whether the MT pole was acquired before or after a rotation, we compared our MT section-mean poles to those predicted from the APWPs of Torsvik et al. (2012), Besse and Courtillot (2002), and Kent and Irving (2010). Specifically, we focused the comparison on those Mesozoic poles furthest east and most likely to be similar to the rotated MT pole (Table 1). We applied Watson's *V* statistic test for a common mean (Watson, 1983; Tauxe et al., 2010). For each APWP pole, the MT direction passed the test for a common mean if it was acquired after the rotation, but failed the test for a common mean if it was acquired before the rotation (supplementary Table S6 [see footnote 1]). Statistically, the MT pole is similar to poles ranging from 136.8 to 3.0 Ma in age, but as we suggest that it is an overprint acquired during the Cordilleran orogeny, that constrains it to be likely older than the Late Cretaceous. Additionally, as our MT direction has a reversed polarity, it cannot have been obtained during the Cretaceous normal polarity superchron (120.6–83.0 Ma; Gee and Kent, 2007). Thus, the MT pole is due to greenschist metamorphism acquired either between 136.8 and 120.6 Ma, or after 83.0 Ma but before the end of Cordilleran metamorphism, and the large-scale rotation was completed by this time. Finally, the LT pole is similar to the present-day field, and given its low unblocking temperature, it is likely a recent viscous remanent magnetization (VRM).

Geological Context of Rotation

The paleomagnetic data presented here suggest that the Mount Harper volcanics rotated relative to the Laurentian craton sometime after the eruption of the Mount Harper volcanics (Neoproterozoic) and before the acquisition of the MT overprint (Mesozoic). There are several possible scenarios for the scale of this rotation: (1) local block rotation of the Mount Harper volcanics, (2) regional rotation of the Coal Creek inlier, and (3) a greater rotation of the Yukon block relative to the Laurentian craton. As suggested initially by Roots (1987), the Mount Harper volcanics and accompanying SSE-striking faults may have been rotated counterclockwise between the North and South Harper faults during regional transtension (Fig. 2); however, the observed angles between SSE-striking faults and the North and South Harper faults suggest that only 20° of rotation can be explained by this mechanism, and therefore it is unlikely that a 50° rotation could be accommodated locally. It is possible that the tectonic rotation involved just the greater Coal Creek inlier, but regional geological data (Eisbacher, 1981; Aitken and McMechan, 1992; Abbott, 1996) support wholesale motion between the Yukon block and autochthonous Laurentia. Additionally, there are two scenarios for the timing of the rotation: (1) the rotation occurred between the Carboniferous and Cretaceous, after the HT2 overprint was acquired but before the MT overprint, and (2) the rotation occurred in the Cryogenian–Ediacaran, before the HT2 overprint was acquired.

Geological and Geophysical Constraints on Rotation of the Yukon Block

The restoration of the Yukon block to a pre-rotation position results in alignment of the correlative Bear River dikes (e.g., Schwab et al., 2004) and Mackenzie dike swarm (LeCheminant and Heaman, 1989; Thorkelson et al., 2005), as well as paleocurrent orientations in the correlative Wernecke and Hornby Bay–Dismal Lakes Groups (Aitken and McMechan, 1992). This tectonic rotation also explains the profound differences in Neoproterozoic facies belts and stratigraphy across the Snake River fault between the Wernecke Mountains and the Mackenzie Mountains (Eisbacher, 1981, 1983; Aitken and McMechan, 1992; Abbott, 1996; Thorkelson, 2000). More specifically, distinct strata of the extensive Mackenzie Mountains Supergroup are abruptly truncated at the Snake River fault and are in part represented by strikingly different strata of the Pinguicula, Hematite Creek, and Fifteenmile Groups to the west in Yukon (Eisbacher, 1981; Thorkelson et al., 2005; Turner, 2011; Macdonald et al., 2012). The Windermere Supergroup also shows dramatic facies change across the Snake River fault (Eisbacher, 1981; Gabrielse and Campbell, 1992; Macdonald et al., 2013). Therefore, geologic evidence suggests that large-scale tectonic displacement may have fortuitously juxtaposed the Proterozoic strata of the Wernecke inlier adjacent to cogenetic but not originally contiguous strata of the northern Mackenzie Mountains.

Any displacement or rotation inferred from the Mount Harper volcanics paleomagnetic data should be matched by the orientation of regional basement trends; however, the crystalline basement is not exposed in Yukon. Previous workers have used aeromagnetic data to elucidate the extent of the basement (e.g., Norris and Dyke, 1997; Aspler et al., 2003; Crawford et al., 2010; see cross-hatched area in Fig. 1). The greater Mackenzie region is dominated by a large positive curvilinear magnetic anomaly called the Fort Simpson anomaly to the south, and the Mackenzie River anomaly in the north (Aspler et al., 2003; Cook et al., 2005; Pilkington and Saltus, 2009; Crawford et al., 2010). Although it is possible that the Mackenzie River/Fort Simpson anomaly reflects continuous crystalline basement into the Yukon block, it cannot be demonstrated that it represents a single tectonic entity along its entire length (Brunstein, 2002; Aspler et al., 2003; Cook et al., 2005). In fact, a recent aeromagnetic study of the Wernecke inlier suggests that the present geometry of the Mackenzie River anomaly is partially offset between the Yukon block and the rest of the craton with ~100 km of sinistral displacement (Crawford et al., 2010).

Carboniferous–Cretaceous Rotation, After HT2 Overprint but Before MT Overprint

If the rotation occurred after the HT2 overprint but before the MT overprint, it could be linked to the putative Jurassic–Cretaceous opening of the Canada Basin, during which the Arctic Alaska terrane has been proposed to have rotated ~66° counterclockwise about a pole within the Mackenzie Delta region (Halgedahl and Jarrard, 1987). Despite the apparent similarity of

this proposed large counterclockwise rotation, there are inconsistencies in kinematic models for the opening of the Canada Basin (e.g., Lane, 1997). Furthermore, more recent models for the opening of the Canada Basin suggest a multiphase extensional and rotational history involving a number of smaller tectonic blocks (e.g., Miller et al., 2008; Shephard et al., 2013) or strike-slip motion along the Arctic margin of Canada. Additionally, the collective rotation of Arctic Alaska plus the entire Yukon block is inconsistent with the geometry of structures within northern Yukon (Norris, 1997).

Alternatively, a Mesozoic rotation could be consistent with a potential rotation related to the Ogilvie deflection (Johnston, 2008). The Ogilvie deflection refers to the 90° change in orientation of the boundary between basinal shales (Medial Basin) and platform facies (Ogilvie or Yukon Platform) as well as a change in the strike of the Cordilleran fold-and-thrust belt, from east-west–trending to a north-south orientation in westernmost Yukon (Norris, 1972; Johnston, 2008). If the Ogilvie deflection is original, then the Cretaceous propagation of thrust sheets continuously around a preexisting bend should have resulted in strike-parallel contraction within the hinge region, which is not observed. Additionally, palinspastic restoration of the Mesozoic thrust sheets results in an ~10,000 km "hole," which has been argued as evidence of Cretaceous bending about a vertical axis of rotation of an originally more linear fold-and-thrust belt (Johnston, 2008). If this Cretaceous bending occurred and was involved in our rotation, the scenario requires that HT2 be related to a Silurian–Carboniferous fluid-flow hematization event capable of resulting in a paleomagnetic overprint, and that the creation of the Ogilvie deflection occurred before MT overprint was acquired.

Cryogenian–Ediacaran Rotation, Before HT2 Overprint

Although a Mesozoic rotation of the Yukon block is permissible, previous studies have concluded that the Cambrian–Devonian paleogeographic features are regionally continuous between the Yukon block and North America to the east (Cecile, 1984). Despite deformation along the southern segments of the Richardson fault array, Paleozoic strata such as the mid-Cambrian Slats Creek Formation persist across the fault array with only right-lateral displacement on the order of 10–20 km (Fritz, 1972; Cecile, 1984; Morrow, 1999). By the Late Cambrian, the Bouvette Formation was deposited across the entire Yukon block, and its equivalents are present on the Mackenzie-Peel shelf. In contrast, Proterozoic strata show large disconti-

nuities across the Richardson fault array (e.g., Abbott, 1996). Next, we discuss three intervals of tectonic activity that occurred subsequent to Mount Harper volcanics eruption and prior to Bouvette Formation deposition and could signal the development of this tectonic rotation. This rotation could have been accommodated along a structure or structures between the Yukon block and Mackenzie Mountains.

The first episode, the Cryogenian Hayhook extensional event (Young et al., 1979; Jefferson and Parrish, 1989), was marked by block faulting, uplift, and basinal subsidence during deposition of the lower Windermere Supergroup (Young et al., 1979; Eisbacher, 1981; Jefferson and Parrish, 1989). North-trending normal faults controlled the facies patterns and depositional outline of the basal Windermere Supergroup (pre- to syn-Sayunei Formation of the Rapitan Group; Young et al., 1979; Eisbacher, 1978, 1981, 1985; Jefferson and Parrish, 1989; Norris, 1997). The NNE-trending faults also control the proximal to transitional facies of the Rapitan Group (Eisbacher, 1981, 1985), and although many of the faults are inferred from thickness and facies patterns, some of the synsedimentary paleofault scarps are observed to have distinct stratigraphic offsets and associated alluvial-fan conglomerates (Eisbacher, 1981; Jefferson and Parrish, 1989).

The Hayhook event faults are also associated with tight folds beneath a prominent angular unconformity; for example, in the Nite Creek area (Fig. 1), folds in the Coppercap and Sayunei Formations that are overturned to the west are overlain by flat-lying Shezal Formation glacial deposits (Helmstaedt et al., 1979; Eisbacher, 1981; Yeo, 1984). Further south, in the Thundercloud Range (Fig. 1), a large faulted and overturned anticline-syncline pair underlies an undeformed section of the Shezal Formation (Jefferson and Parrish, 1989). The north-trending tight folds and unconformities are interpreted to represent regional transpressional contraction during the deposition of the Sayunei Formation, followed by an intra-Sayunei unconformity (Helmstaedt et al., 1979; Eisbacher, 1981; Yeo, 1984). In the Wernecke inlier, Thorkelson (2000) observed east-trending normal faults of the Hayhook extensional event that crosscut older, west-verging thrust faults and folds in Sequence B rocks, suggesting that the compressional folds represent an earlier event referred to as the Corn Creek orogeny (1.00–0.78 Ga from Thorkelson et al., 2005). The Corn Creek structures fold the ca. 850–780 Ma Mackenzie Mountains Supergroup (Eisbacher, 1981; Jefferson and Parrish 1989) and are sealed by ca. 660–635 Ma strata (Mount Profeit dolostone of Eisbacher, 1981; Macdonald et al., 2013; Rooney et al., 2014, 2015).

Thus, the Corn Creek structures likely formed between ca. 780 and 635 Ma and could represent transpressional activity related to motion along the Snake River fault. The syn-Rapitan Hayhook extensional event likely reached its peak shortly after the emplacement of the ca. 717 Ma Mount Harper volcanics (Jefferson and Parrish, 1989).

Following the Hayhook extensional event, the next possible time that the Yukon block could have rotated is during the deposition of units overlying the Rapitan Group in the upper Windermere Supergroup, such as the Keele and Ice Brook Formations, and the equivalent Mount Profeit dolostone (Eisbacher, 1981; Aitken, 1991a). Near the Snake River fault in the Wernecke Mountains, sedimentary facies of the Hay Creek Group dramatically change from the massive Mount Profeit dolostone to carbonate olistoliths encased in shale and sandstone turbidites (Eisbacher, 1981; Thorkelson, 2000). The olistolith-bearing succession is overlain by a thick package of siliciclastic turbidites (Eisbacher, 1981). Eisbacher (1981) related these dramatic facies changes to synsedimentary tectonism along the Snake River fault zone. A similar pattern is seen west of the Plateau thrust in the central Mackenzie Mountains, where platformal carbonates of the Keele Formation "break away" into olistoliths and overlying turbidites of the Durkan and Delthore Members of the Ice Brook Formation (Aitken, 1991a, 1991b). The Durkan and Delthore Members of the Ice Brook Formation are locally overlain by glacial diamictite of the Stelfox Member (Aitken, 1991a, 1991b), along with overlying carbonate of the Ediacaran Ravensthroat Formation, which are correlative with the Marinoan glaciation and associated cap carbonates, respectively (Young, 1995; James et al., 2001). This correlation suggests that any tectonic activity associated with the dramatic facies changes must have been initiated after 662.4 ± 3.9 Ma (base of the Twitya; Rooney et al., 2014) and finished by the deposition of the 632.6 ± 6.3 Ma Sheepbed Formation (Rooney et al., 2015).

Finally, the rotation could have occurred during the deposition of the Ediacaran to Early Cambrian informal "Upper" group (divided into four major depositional sequences that include the following formations and informal units: Sheepbed, Sheepbed carbonate, June beds, Gametrail, Blueflower, and Risky) and Backbone Ranges Formation, specifically during deposition of the June beds (Aitken, 1989; Dalrymple and Narbonne, 1996; MacNaughton et al., 2000, 2008; Pyle et al., 2004; Macdonald et al., 2013). Previously, June bed strata were interpreted as Sheepbed-equivalent slope deposits characterized by debris flows and turbidites

(Dalrymple and Narbonne, 1996); however, the abrupt appearance of poorly sorted and coarse-grained sandstone and conglomerate units within the lower June beds, and the regional documentation of rapid facies changes from northeast to southwest in the central Mackenzie Mountains and the Wernecke Mountains suggest synsedimentary tectonism during "Upper" group sedimentation (Macdonald et al., 2013; Moynihan, 2014). Ediacaran fossils in the June beds can be correlated globally with the ca. 580–560 Ma Avalon assemblage (Narbonne and Aitken, 1990; Narbonne, 1994; Gehling et al., 2000; Narbonne and Gehling, 2003; Narbonne et al., 2012). This ca. 580–560 Ma age for the June beds would place the possible syntectonic event coincident with the ca. 570 Ma synrift volcanics preserved in the southern Canadian Cordillera (Colpron et al., 2002) and with thermal subsidence models (e.g., Bond and Kominz, 1984) that indicate latest Ediacaran rifting on the western margin of Laurentia.

Neoproterozoic Paleogeographic Implications

This rotation has implications for the interpretation of the Neoproterozoic stratigraphy and structures in the Coal Creek inlier and their bearing on the breakup of Rodinia. In its present position, with the assumption that the Yukon block has not rotated, the pre–811 Ma WSW-ENE structures in the Fifteenmile Group suggest north-directed extension on the northern margin of Laurentia (Macdonald et al., 2012). Additionally, syn-Windermere extensional structures involve a 120° bend in orientation from the Mackenzie Mountains to the Coal Creek inlier, with southwest-oriented extension in Mackenzie Mountains and north-directed extension in Yukon. With the rotation, pre–811 Ma WSW-ENE structures in the Fifteenmile Group rotate roughly parallel to the strike of the Mackenzie arc (Aitken and Long, 1978) and could be related to east-west–directed extension of an aulacogen related to the deposition of the Mackenzie Mountain Supergroup to the east. Restoration of the Yukon block to its prerotation position also aligns extensional structures of the Coal Creek and Hart River inliers with those of the NW Mackenzie Mountains, as well as connecting Mount Harper Group embayments to asymmetrical extensional half grabens in the Coates Lake Group of the Mackenzie Mountains (Strauss et al., 2015).

Here, we integrate our data from Laurentia into a recent model of Rodinia put forth by Li et al. (2013). Our preferred model of counter-clockwise rotation of the Yukon block with respect to Laurentia is consistent with Neo-

proterozoic Laurentian tectonic events divided into three main phases. First, prior to this putative rotation, a NNW-trending (present-day coordinates) failed rift developed during early Neoproterozoic extension along the northern margin of Laurentia (Aitken, 1981; Macdonald et al., 2012). With this failed rift, the pre–811 Ma WSW- and ENE-oriented structures in the Fifteenmile Group of the Coal Creek inlier could represent conjugate structures to the extensional structures in the Mackenzie Mountain Supergroup, rather than orthogonal extension on the northwest margin of Laurentia (e.g., Turner and Long, 2008). During the second phase, syn-Windermere extension resulted in opposing asymmetrical extensional half grabens in the Coal Creek inlier and the Mackenzie Mountains (Figs. 8A and 8C) with the eruption of the Mount Harper volcanics coincident with the emplacement of the Franklin LIP. Synmagmatic extension associated with the Franklin LIP could have been related to rifting on the northern margin of Laurentia (Pisarevsky et al., 2013; Rainbird, 1993).

The development of smaller extensional structures (e.g., the north-south–trending Mount Harper fault) orthogonal to larger, margin-scale rifting is a common feature during opening of ocean basins such as in Africa during the opening of the South Atlantic, in which rifting along the future continental margins was accompanied by activity in basins trending orthogonal to that dominant rift expression (Maurin and Guiraud, 1990; Guiraud and Maurin, 1992). Finally, we suggest that the Yukon block rotated counter-clockwise during either one or more of the following events: the Cryogenian Hayhook event, deposition of the Cryogenian Keele and Ice Brook Formations and equivalent Mount Profeit dolostone, or the Ediacaran to Early Cambrian deposition of the informal "Upper" group and Backbone Ranges Formation (Figs. 8B and 8D).

It is possible that, in addition to this rotation, the Yukon block may have experienced large-scale translation relative to stable Laurentia, potentially localized along the Snake River fault. Although the folding and unconformities in the Wernecke and Mackenzie Mountains have previously been interpreted to represent regional transpression during the deposition of the Sayunei Formation (Helmstaedt et al., 1979; Eisbacher, 1981), there are few constraints on the nature of lateral displacements. If the counter-clockwise rotation was coincident with a translation, it would have occurred within a sinistral strike-slip system. Eisbacher (1983) initially proposed sinistral displacement between the Yukon block and Laurentia, although he suggested a Devonian age for the displacement that was later called into question based on geological grounds

by Cecile (1984). An analogous tectonic rotation would be the >60° clockwise rotation of the Transverse Ranges of the southwestern United States during early development of the San Andreas fault system (Jackson and Molnar, 1990). In addition, some amount of sinistral translation seems consistent with displacements observed in the aeromagnetic data (Pilkington and Saltus, 2009; Crawford et al., 2010).

Low-Latitude Glaciation

The snowball Earth hypothesis suggests that Neoproterozoic glaciations were global and synchronous at low latitudes (Hoffman et al., 1998; Hoffman and Schrag, 2002). The geochronological correlation between the Mount Harper volcanics and the Franklin LIP suggests that the glaciogenic Rapitan Group equivalent in the Coal Creek inlier was deposited at low latitudes (Macdonald et al., 2010), and this has been used as the highest-reliability evidence for the low-latitude nature of the Sturtian glaciation (Evans and Raub, 2011). However, the paleolatitude predicted for the Mount Harper volcanics from the Franklin LIP paleomagnetic data (21° ± 3° *in* Evans and Raub, 2011; or 19.3° ± 3° using the D+90can pole of Denyszyn et al., 2009a) is higher than the previous estimates of paleolatitude for the Sturtian glaciation (Park, 1997; Evans, 2000; Evans and Raub, 2011). The paleomagnetic poles from the Rapitan Group (Morris, 1977; Park, 1997) suggest very low-latitude (6° ± 4° and 4° ± 6°) glaciogenic sedimentation; however, it is uncertain if these poles are primary (e.g., Evans, 2000). As the Mount Harper volcanics interfinger with glaciogenic Sturtian deposits, these paleomagnetic data are well suited to better understand the low-latitude nature of these deposits. The paleomagnetic data from previous study of the Mount Harper volcanics resulted in very low paleolatitudes of 3° ± 12° (Park et al., 1992) and substantial overlap between the Yukon block and Laurentia. Using our HT1 pole, the Mount Harper volcanics restores to a paleolatitude of 24.3° ± 13.8°. This is consistent with the interpretation that the age from member D of the Mount Harper volcanic complex provides a maximum age constraint on the low-latitude Sturtian glaciation and the Mount Harper volcanics–Rapitan Group equivalent sequence provides a unique exposure that captures the transition into glacial conditions of the Sturtian glaciation, after which ice advanced extremely rapidly to the equator. Here, we provide a paleolatitude for volcanics that were emplaced immediately before and during deposition of the Rapitan Group that indicates low latitude (<30°) ca. 717 Ma, i.e., at the beginning of the Sturtian glaciation.
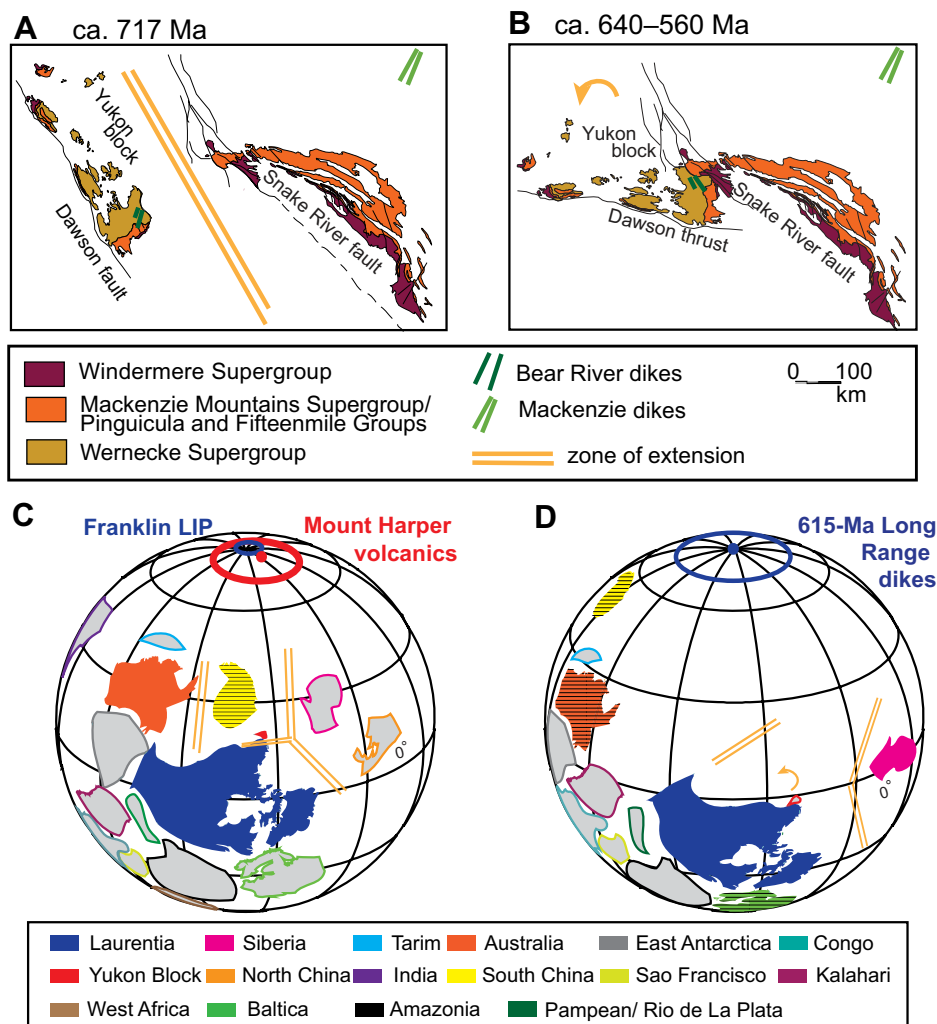
Figure 8. Top: Change in orientation with time of the Proterozoic inliers, where black boxes match the extent of the Figure 1 map of northwest Canada with Proterozoic inliers. The orientation of the Bear River dikes in the Wernecke inlier and the correlative Mackenzie dike swarm on the Laurentian craton are represented with green lines in their approximate geographic location and orientation. (A) The Yukon block restored to its position prior to tectonic rotation. (B) The Yukon block in its present-day position. Bottom: Paleogeographic reconstructions that incorporate the tectonic block rotation of the Yukon block into the context of the rifting of Rodinia. The reconstructions are modified slightly from those Li et al. (2013). The pole for the Long Range dikes is from Buchan (2014). Brightly colored continents are those with paleomagnetic data within 5 m.y. of the reconstructed time. Continents overlain with horizontal lines are those with paleomagnetic data within 30 m.y. of the reconstructed time. Continents in gray with colored outlines lack paleomagnetic data within 30 m.y. to support any reconstruction for that time. Steps in the reconstruction: (C) Following the development of an aulacogen and rifting on the northern margin, the Mount Harper volcanics (MHV) and Franklin large igneous province (LIP) erupt ca. 717 Ma. (D) The Yukon block rotates counterclockwise relative to Laurentia. Subsequently, Ediacaran rifting commences on the western margin of Laurentia.

CONCLUSIONS

We confirm the presence of a Mount Harper volcanics pole 50° away from the expected 721–712 Ma Laurentian Franklin pole of Denyszyn et al. (2009a). The paleomagnetic direction identified and used to create the reconstructions presented here does have some issues, most notably that the HT1 direction is not ubiquitous in the Mount Harper volcanics, but it is based on data from five sections. Additionally, we suggest that we have captured secular variation in our primary pole, although we lack definitive evidence. Despite these limitations, the primary nature of this paleomagnetic direction is supported by six of the seven Van der Voo (1990) reliability criteria. Finally, we acknowledge that the paleomagnetic data do not provide firm constraints on the timing of the rotation, only that the rotation occurred after the eruption of the Mount Harper volcanics and before the MT overprint was acquired. Although a Mesozoic rotation of the Yukon block is permissible, the abundance of potential overprint events in the Neoproterozoic and Cambrian compared to the later Paleozoic suggests that the rotation occurred during the Early Cambrian or Neoproterozoic. We explain the paleomagnetic data via the following sequence of events. First, the Mount Harper volcanics erupted, and two reversals were captured during volcanism. Synvolcanic normal displacement along the Mount Harper fault resulted in the development of the Mount Harper synform. Although volcanism and the development of the synform were occurring at the same time, the magnetization was acquired on much shorter time scales, resulting in passage of the fold test and a prefolding, synvolcanic, primary magnetization for HT1. Second, the Yukon block and the Mount Harper volcanics rotated 50° counterclockwise relative to autochthonous Laurentia. Regional geological considerations suggest this rotation may have been Cryogenian to early Paleozoic in age. Either before or after this rotation, fluid flow and hematization events resulted in the HT2 chemical overprint. Next, during the Cordilleran orogeny, Cretaceous greenschist metamorphism imparted the MT thermal overprint. Finally, the recently acquired LT VRM overprint records the present-day geomagnetic field.

Northwest Laurentia records the complex breakup of Rodinia. Vertical-axis tectonic block rotations can complicate interpretations of this geological history; however, identifying and restoring those rotations may also provide insight into earlier tectonics. With the rotation presented herein, the WSW-ENE structures of the early Neoproterozoic basin-forming events (Sequence B of Young et al., 1979) on the Yukon block represent the conjugate margin of a extensional system formed opposite of the Mackenzie Mountain Supergroup basin, rather than extension on the northwest margin of Laurentia. In addition, the HT1 pole from the Mount Harper volcanics is a low-latitude pole from volcanic units that interfinger with deposits from the Sturtian glaciation, thus adding more evidence in favor of a global snowball Earth event at ca. 717 Ma.

ACKNOWLEDGMENTS

REFERENCES CITED

Abbott, J.G., 1996, Implications of probable late Proterozoic dextral strike-slip movement on the Snake River fault, *in* Cook, F.A., and Erdmer, P., eds., Slave–Northern Cordillera Lithospheric Evolution (SNORCLE) Transect: Lithoprobe Report 50, p. 138–140.

Abbott, G., 1997, Geology of the Upper Hart River Area, Eastern Ogilvie Mountains, Yukon Territory (116A/10, 116A/11): Exploration and Geological Services Division, Yukon, Indian and Northern Affairs Canada Bulletin 9, 92 p.

Aitken, J.D., 1981, Stratigraphy and sedimentology of the Upper Proterozoic Little Dal Group, Mackenzie Mountains, Northwest Territories, *in* Campbell, F.H.A., ed., Proterozoic Basins of Canada: Geological Survey of Canada Paper 81-10, p. 47–71.

Aitken, J.D., 1989, Uppermost Proterozoic Formations in Central Mackenzie Mountains, Northwest Territories: Geological Survey of Canada Bulletin 368, 26 p., doi: 10.4095/126611.

Aitken, J.D., 1991a, The Ice Brook Formation and Post-Rapitan, Late Proterozoic Glaciation, Mackenzie Mountains, Northwest Territories: Geological Survey of Canada Bulletin 404, p. 1–43, doi:10.4095/132664.

Aitken, J.D., 1991b, Two late Proterozoic glaciations, Mackenzie Mountains, northwestern Canada: Geology, v. 19, no. 5, p. 445–448, doi:10.1130/0091-7613(1991)019<0445:TLPGMM>2.3.CO;2.

Aitken, J.D., 1993, Tectonic evolution and basin history, *in* Stott, D.E., and Aitken, J.D., eds., Sedimentary Cover of the North American Craton in Canada: Geological Survey of Canada, Geology of Canada 5, p. 483–504.

Aitken, J.D., and Long, D.G.F., 1978, Mackenzie tectonic arc—Reflection of early basin configuration?: Geology, v. 6, p. 626–629, doi:10.1130/0091-7613(1978)6<626:MTAOEB>2.0.CO;2.

Aitken, J.D., and McMechan, M.E., 1992, Middle Proterozoic assemblages, *in* Gabrielse, H., and Yorath, C.J., eds., Geology of the Cordilleran Orogen in Canada: Geological Survey of Canada, Geology of Canada 4, p. 97–124 (also Geological Society of America, The Geology of North America, v. G-2).

Aspler, L.B., Pilkington, M., and Miles, W.F., 2003, Interpretations of Precambrian basement based on recent aeromagnetic data, Mackenzie Valley, Northwest Territories: Geological Survey of Canada, Current Research 2003-C2, 11 p., doi:10.4095/214184.

Banerjee, S.K., 1971, New grain size limits for paleomagnetic stability in hematite: Nature. Physical Science (London), v. 232, p. 15–16, doi:10.1038/physci232015a0.

Besse, J., and Courtillot, V., 2002, Apparent and true polar wander and the geometry of the geomagnetic field over the last 200 Myr: Journal of Geophysical Research, v. 107, no. B11, p. EPM 6-1–EPM 6-31, doi:10.1029/2000JB000050.

Bond, G.C., and Kominz, M.A., 1984, Construction of tectonic subsidence curves for the early Paleozoic miogeocline, southern Canadian Rocky Mountains: Implications for subsidence mechanisms, age of breakup, and crustal thinning: Geological Society of America Bulletin, v. 95, no. 2, p. 155, doi:10.1130/0016-7606(1984)95<155:COTSCF>2.0.CO;2.

Brunstein, F.C., ed., 2002, Magnetic Anomaly Map of North America: Denver, Colorado, U.S. Geological Survey, scale 1:10,000,000.

Buchan, K.L., 2014, Reprint of "Key paleomagnetic poles and their use in Proterozoic continent and supercontinent reconstructions: A review": Precambrian Research, v. 244, p. 5–22, doi:10.1016/j.precamres.2014.01.010.

Buchan, K.L., and Ernst, R.E., 2004, Diabase Dyke Swarms and Related Units in Canada and Adjacent Regions: Geological Survey of Canada Map 2022A, scale 1:5,000,000, with accompanying compilation, 39 p.

Buchan, K.L., and Ernst, R.E., 2013, Diabase Dyke Swarms of Nunavut, Northwest Territories and Yukon, Canada: Geological Survey of Canada Open-File 7464, 24 p., doi:10.4095/293149.

Buchan, K.L., Mertanen, S., Park, R.G., Pesonen, L.J., Elming, S.Å., Abrahamsen, N., and Bylund, G., 2000, Comparing the drift of Laurentia and Baltica in the Proterozoic: The importance of key palaeomagnetic poles: Tectonophysics, v. 319, no. 3, p. 167–198, doi:10.1016/S0040-1951(00)00032-9.

Buchan, K.L., Ernst, R.E., Bleeker, W., Davis, W.J., Villeneuve, M., van Breemen, O., Hamilton, M.A., and Suderlund, U., 2010, Proterozoic Magmatic Events of the Slave Craton, Wopmay Orogen and Environs: Geological Survey of Canada Open-File 5985, 25 p., doi: 10.4095/285383.

Butler, R.F., 1992, Paleomagnetism: Magnetic Domains to Geologic Terranes: Boston, Massachusetts, Blackwell Scientific Publications, 238 p.

Camp, V.E., Ross, M.E., and Hanson, W.E., 2003, Genesis of flood basalts and Basin and Range volcanic rocks from Steens Mountain to the Malheur River Gorge, Oregon: Geological Society of America Bulletin, v. 115, no. 1, p. 105–128, doi:10.1130/0016-7606(2003)115<0105:GOFBAB>2.0.CO;2.

Cecile, M.P., 1984, Evidence against large-scale strike-slip separation of Paleozoic strata along the Richardson-Hess fault system, northern Canadian Cordillera: Geology, v. 12, no. 7, p. 403–407, doi:10.1130/0091-7613(1984)12<403:EALSSO>2.0.CO;2.

Cecile, M.P., Morrow, D.W., and Williams, G.K., 1997, Early Paleozoic (Cambrian to Early Devonian) tectonic framework, Canadian Cordillera: Bulletin of Canadian Petroleum Geology, v. 45, no. 1, p. 54–74.

Christie, K.W., and Fahrig, W.F., 1983, Paleomagnetism of the Borden dykes of Baffin Island and its bearing on the Grenville Loop: Canadian Journal of Earth Sciences, v. 20, no. 2, p. 275–289, doi:10.1139/e83-025.

Cisowski, S., 1981, Interacting vs. non-interacting single domain behavior in natural and synthetic samples: Physics of the Earth and Planetary Interiors, v. 26, p. 56–62, doi: 10.1016/0031-9201(81)90097-2.

Colpron, M., Logan, J., and Mortensen, J., 2002, U-Pb zircon age constraint for late Neoproterozoic rifting and initiation of the Lower Paleozoic passive margin of western Laurentia: Canadian Journal of Earth Sciences, v. 39, no. 2, p. 133–143, doi:10.1139/e01-069.

Cook, F.A., Hall, K.W., and Lynn, C.E., 2005, The edge of northwestern North America at ~1.8 Ga: Canadian Journal of Earth Sciences, v. 42, no. 6, p. 983–997, doi: 10.1139/e05-039.

Cox, G.M., 2015, Linking Tectonics, LIP Emplacement and Environmental Change in the Cryogenian [Ph.D. thesis]: Montreal, McGill University, 301 p.

Cox, G.M., Roots, C.F., Halverson, G.P., Minarik, W.G., Macdonald, F.A., and Hubert-Theou, L., 2013, Mount Harper volcanic complex, Ogilvie Mountains: A far-flung occurrence of the Franklin igneous event?, *in* MacFarlane, K.E., Nordling, M.G., and Sack, P.J., eds., Yukon Exploration and Geology 2012: Whitehorse, Yukon Geological Survey, p. 19–36.

Crawford, B.L., Betts, P.G., and Aillères, L., 2010, An aeromagnetic approach to revealing buried basement structures and their role in the Proterozoic evolution of the Wernecke Inlier, Yukon Territory, Canada: Tectonophysics, v. 490, no. 1–2, p. 28–46, doi:10.1016/j.tecto.2010.04.025.

Dalrymple, R.W., and Narbonne, G.M., 1996, Continental slope sedimentation in Sheepbed Formation (Neoproterozoic, Windermere Supergroup), Mackenzie Mountains, N.W.T.: Canadian Journal of Earth Sciences, v. 33, no. 6, p. 848–862, doi:10.1139/e96-064.

Dalziel, I.W.D., 1997, Neoproterozoic–Paleozoic geography and tectonics: Review, hypothesis, environmental speculation: Geological Society of America Bulletin, v. 109, no. 1, p. 16–42, doi:10.1130/0016-7606(1997)109<0016:ONPGAT>2.3.CO;2.

Deenen, M.H., Langereis, C.G., van Hinsbergen, D.J., and Biggin, A.J., 2011, Geomagnetic secular variation and the statistics of palaeomagnetic directions: Geophysical Journal International, v. 186, no. 2, p. 509–520, doi: 10.1111/j.1365-246X.2011.05050.x.

Delaney, G.D., 1981, The mid-Proterozoic Wernecke Supergroup, Wernecke Mountains, Yukon Territory, *in* Campbell, F.H.A., ed., Proterozoic Basins of Canada: Geological Survey of Canada Paper 81-10, p. 1–23.

Denyszyn, S.W., Halls, H.C., Davis, D.W., and Evans, D.A., 2009a, Paleomagnetism and U-Pb geochronology of Franklin dykes in High Arctic Canada and Greenland: A revised age and paleomagnetic pole constraining block rotations in the Nares Strait region: Canadian Journal of Earth Sciences, v. 46, no. 9, p. 689–705.

Denyszyn, S.W., Davis, D.W., and Halls, H.C., 2009b, Paleomagnetism and U-Pb geochronology of the Clarence Head dykes, Arctic Canada: Orthogonal emplacement of mafic dykes in a large igneous province: Canadian Journal of Earth Sciences, v. 46, no. 3, p. 155–167, doi: 10.1139/E09-011.

Dunlop, D.J., 2002, Theory and application of the Day plot (Mrs/Ms versus Hcr/Hc), 1. Theoretical curves and tests using titanomagnetite data: Journal of Geophysical Research, v. 107, no. B3, p. EPM 4-1–EPM 4-22.

Dunlop, D.J., and Buchan, K.L., 1977, Thermal remagnetization and the paleointensity record of metamorphic rocks: Physics of the Earth and Planetary Interiors, v. 13, no. 4, p. 325–331, doi:10.1016/0031-9201(77)90117-0.

Eisbacher, G.H., 1978, Redefinition and Subdivision of the Rapitan Group, Mackenzie Mountains: Geological Survey of Canada Paper 77-35, 21 p., doi:10.4095/103527.

Eisbacher, G.H., 1981, Sedimentary Tectonics and Glacial Record in the Windermere Supergroup, Mackenzie Mountains, Northwestern Canada: Geological Survey of Canada Paper 80-27, 40 p., doi:10.4095/119453.

Eisbacher, G.H., 1983, Devonian-Mississippian sinistral transcurrent faulting along the cratonic margin of western North America: A hypothesis: Geology, v. 11, no. 1, p. 7–10, doi:10.1130/0091-7613(1983)11<7:DSTFAT>2.0.CO;2.

Eisbacher, G.H., 1985, Late Proterozoic rifting, glacial sedimentation, and sedimentary cycles in the light of Windermere deposition, western Canada: Palaeogeography, Palaeoclimatology, Palaeoecology, v. 51, no. 1–4, p. 231–254, doi:10.1016/0031-0182(85)90087-2.

Ernst, R.E., Hamilton, M.A., Söderlund, U., Hanes, J.A., Gladkochub, D.P., Okrugin, A.V., Kolotilina, T., Mekhonoshin, A.S., Bleeker, W., LeCheminant, A.N., Buchan, K.L., Chamberlain, K.R., and Didenko, A.N., 2016, Long-lived connection between southern Siberia and northern Laurentia in the Proterozoic: Nature Geoscience, v. 9, p. 464–469, doi:10.1038/ngeo2700.

Evans, D.A.D., 2000, Stratigraphic, geochronological, and paleomagnetic constraints upon the Neoproterozoic climatic paradox: American Journal of Science, v. 300, no. 5, p. 347–433, doi:10.2475/ajs.300.5.347.

Evans, D.A.D., 2009, The palaeomagnetically viable, long-lived and all-inclusive Rodinia supercontinent reconstruction, *in* Murphy, J.B., Keppie, J.D., and Hynes, A.J., eds., Ancient Orogens and Modern Analogues: Geological Society of London Special Publication 327, p. 371–404, doi:10.1144/SP327.16.

Evans, D.A.D., and Raub, T.D., 2011, Neoproterozoic glacial palaeolatitudes: A global update, *in* Arnaud, E., Halverson, G.P., and Shields-Zhou, G., eds., The Geological

Record of Neoproterozoic Glaciations: Geological Society of London Memoir 36, p. 93–112.

Ewart, A., Schon, R.W., and Chappell, B.W., 1992, The Cretaceous volcanic-plutonic province of the central Queensland (Australia) coast—A rift-related 'calc-alkaline' province, *in* Brown, P.E., and Chappell, B.W., eds., The Second Hutton Symposium: The Origin of Granites and Related Rocks: Geological Society of America Special Paper 272, p. 327–346.

Fahrig, W.F., and Schwarz, E.J., 1973, Additional paleomagnetic data on the Baffin diabase dikes and a revised Franklin pole: Canadian Journal of Earth Sciences, v. 10, no. 4, p. 576–581, doi:10.1139/e73-057.

Fahrig, W.F., Irving, E., and Jackson, G.D., 1971, Paleomagnetism of the Franklin diabases: Canadian Journal of Earth Sciences, v. 8, no. 4, p. 455–467, doi:10.1139/e71-047.

Fan, W.M., Guo, F., Wang, Y.J., and Lin, G., 2003, Late Mesozoic calc-alkaline volcanism of post-orogenic extension in the northern Da Hinggan Mountains, northeastern China: Journal of Volcanology and Geothermal Research, v. 121, no. 1–2, p. 115–135, doi:10.1016/S0377-0273(02)00415-8.

Fritz, W.H., 1972, Lower Cambrian Trilobites from the Sekwi Formation Type Section, Mackenzie Mountains, Northwestern Canada: Geological Survey of Canada Bulletin 212, 90 p., doi:10.4095/100784.

Fu, X., Zhang, S., Li, H., Ding, J., Li, H., Yang, T., Wu, H., Yuan, H., and Lv, J., 2015, New paleomagnetic results from the Huaibei Group and Neoproterozoic mafic sills in the North China craton and their paleogeographic implications: Precambrian Research, v. 269, p. 90–106, doi:10.1016/j.precamres.2015.08.013.

Furlanetto, F., Thorkelson, D.J., Gibson, H.D., Marshall, D.D., Rainbird, R.H., Davis, W.J., Crowley, J.L., and Vervoort, J.D., 2013, Late Paleoproterozoic terrane accretion in northwestern Canada and the case for circum-Columbian orogenesis: Precambrian Research, v. 224, p. 512–528, doi:10.1016/j.precamres.2012.10.010.

Gabrielse, H., 1967, Tectonic evolution of the northern Canadian Cordillera: Canadian Journal of Earth Sciences, v. 4, no. 2, p. 271–298, doi:10.1139/e67-013.

Gabrielse, H., and Campbell, R.B., 1992, Upper Proterozoic assemblages, *in* Gabrielse, H., and Yorath, C.J., eds., Geology of the Cordilleran Orogen in Canada: Geological Survey of Canada, Geology of Canada 4, Chap. 6, p. 127–150 (also Geological Society of America, The Geology of North America, v. G-2).

Gans, P.B., Mahood, G.A., and Schermer, E., 1989, Synextensional Magmatism in the Basin and Range Province; a Case Study from the Eastern Great Basin: Geological Society of America Special Paper 233, 53 p., doi:10.1130/SPE233-p1.

Gawthorpe, R.L., and Leeder, M.R., 2000, Tectono-sedimentary evolution of active extensional basins: Basin Research, v. 12, no. 3–4, p. 195–218, doi:10.1046/j.1365-2117.2000.00121.x.

Gee, J.S., and Kent, D.V., 2007, Source of oceanic magnetic anomalies and the geomagnetic polarity time scale, *in* Schubert, G., ed., Treatise on Geophysics, Volume 5: Geomagnetism: Amsterdam, Netherlands, Elsevier, p. 455–507.

Gehling, J.G., Narbonne, G.M., and Anderson, M.A., 2000, The first named Ediacaran body fossil, *Aspidella terranovica*: Palaeontology, v. 43, p. 427–456, doi:10.1111/j.0031-0239.2000.00134.x.

Geissman, J.W., and Harlan, S.S., 2002, Late Paleozoic remagnetization of Precambrian crystalline rocks along the Precambrian/Carboniferous nonconformity, Rocky Mountains: A relationship among deformation, remagnetization, and fluid migration: Earth and Planetary Science Letters, v. 203, no. 3–4, p. 905–924, doi:10.1016/S0012-821X(02)00932-9.

Goddéris, Y., Donnadieu, Y., Nedelec, A., Dupre, B., Dessert, C., Grard, A., Ramstein, G., and Francois, L.M., 2003, The Sturtian 'snowball' glaciation: Fire and ice: Earth and Planetary Science Letters, v. 211, no. 1–2, p. 1–12, doi:10.1016/S0012-821X(03)00197-3.

Goodfellow, W., Cecile, M., and Leybourne, M., 1995, Geochemistry, petrogenesis, and tectonic setting of Lower Paleozoic alkalic and potassic volcanic rocks, northern

Canadian Cordilleran miogeocline: Canadian Journal of Earth Sciences, v. 32, no. 8, p. 1236–1254, doi:10.1139/e95-101.

Greenwood, H.J., Woodsworth, G.J., Reed, P.B., Ghent, E.D., and Evenchick, C.A., 1991, Metamorphism, *in* Gabrielse, H., and Yorath, C.J., eds., Geology of the Cordilleran Orogen in Canada: Geological Survey of Canada, Geology of Canada 4, p. 533–570.

Guiraud, R., and Maurin, J.C., 1992, Early Cretaceous rifts of western and central Africa: An overview: Tectonophysics, v. 213, no. 1–2, p. 153–168, doi:10.1016/0040-1951(92)90256-6.

Halgedahl, S.L., and Jarrard, R.D., 1987, Paleomagnetism of the Kuparuk River Formation from oriented drill core: Evidence for rotation of the Arctic Alaska plate, *in* Tailleurc, I., and Weimer, P., eds., Alaskan North Slope Geology: Society of Economic Paleontologists and Mineralogists, Pacific Section, Special Publication 50, p. 581–620.

Hawkesworth, C., Turner, S., Gallagher, K., Hunter, A., Bradshaw, T., and Rogers, N., 1995, Calc-alkaline magmatism, lithospheric thinning and extension in the Basin and Range: Journal of Geophysical Research–Solid Earth, v. 100, no. B6, p. 10,271–10,286, doi:10.1029/94JB02508.

Heaman, L., LeCheminant, A., and Rainbird, R., 1992, Nature and timing of Franklin igneous events, Canada: Implications for a late Proterozoic mantle plume and the break-up of Laurentia: Earth and Planetary Science Letters, v. 109, p. 117–131, doi:10.1016/0012-821X(92)90078-A.

Helmstaedt, H., Eisbacher, G.H., and McGregor, H., 1979, Copper mineralization near an intra-Rapitan unconformity, Nite copper prospect, Mackenzie Mountains, Northwest Territories, Canada: Canadian Journal of Earth Sciences, v. 16, no. 1, p. 50–59, doi:10.1139/e79-005.

Hoffman, P.F., 1991, Did the breakout of Laurentia turn Gondwanaland inside-out?: Science, v. 252, no. 5011, p. 1409–1412, doi:10.1126/science.252.5011.1409.

Hoffman, P.F., and Schrag, D.P., 2002, The snowball Earth hypothesis: Testing the limits of global change: Terra Nova, v. 14, no. 3, p. 129–155, doi:10.1046/j.1365-3121.2002.00408.x.

Hoffman, P.F., Kaufman, A.J., Halverson, G.P., and Schrag, D.P., 1998, A Neoproterozoic snowball Earth: Science, v. 281, no. 5381, p. 1342–1346, doi:10.1126/science.281.5381.1342.

Hooper, P.R., Bailey, D.G. and Holder, G.A., 1995, Tertiary calc-alkaline magmatism associated with lithospheric extension in the Pacific Northwest: Journal of Geophysical Research, Solid Earth, v. 100, no. B6, p. 10,303–10,319.

Irving, E., and Thorkelson, D.J., 1990, On determining paleohorizontal and latitudinal shifts: Paleomagnetism of Spences Bridge Group, British Columbia: Journal of Geophysical Research–Solid Earth, v. 95, no. B12, p. 19,213–19,234, doi:10.1029/JB095iB12p19213.

Jackson, J., and Molnar, P., 1990, Active faulting and block rotations in the western Transverse Ranges, California: Journal of Geophysical Research–Solid Earth (1978–2012), v. 95, no. B13, p. 22,073–22,087.

Jackson, M., 1990, Diagenetic sources of stable remanence in remagnetized Paleozoic cratonic carbonates: A rock magnetic study: Journal of Geophysical Research–Solid Earth, v. 95, no. B3, p. 2753–2761, doi:10.1029/JB095iB03p02753.

James, N.P., Narbonne, G.M., and Kyser, T.K., 2001, Late Neoproterozoic cap carbonates: Mackenzie Mountains, northwestern Canada: Precipitation and global glacial meltdown: Canadian Journal of Earth Sciences, v. 38, no. 8, p. 1229–1262, doi:10.1139/e01-046.

Jefferson, C.W., and Parrish, R.R., 1989, Late Proterozoic stratigraphy, U-Pb zircon ages, and rift tectonics, Mackenzie Mountains, northwestern Canada: Canadian Journal of Earth Sciences, v. 26, no. 9, p. 1784–1801, doi:10.1139/e89-151.

Jeletsky, J.A., 1962, Pre-Cretaceous Richardson Mountains Trough—Its place in the tectonic framework of Arctic Canada and its bearing on some geosynclinals concepts: Transactions of the Royal Society of Canada, v. 56, no. 3, p. 55–84.

Johnson, C.L., and Constable, C.G., 1995, The time-averaged geomagnetic field as recorded by lava flows over the past 5 Myr: Geophysical Journal International, v. 122, no. 2, p. 489–519, doi:10.1111/j.1365-246X.1995.tb07010.x.

Johnston, S.T., 2008, The Cordilleran ribbon continent of North America: Annual Review of Earth and Planetary Sciences, v. 36, p. 495–530, doi:10.1146/annurev.earth.36.031207.124331.

Jones, C., 2002, User-driven integrated software lives: "PaleoMag" paleomagnetics analysis on the Macintosh: Computers & Geosciences, v. 28, no. 10, p. 1145–1151, doi:10.1016/S0098-3004(02)00032-8.

Kent, D.V., and Irving, E., 2010, Influence of inclination error in sedimentary rocks on the Triassic and Jurassic apparent pole wander path for North America and implications for Cordilleran tectonics: Journal of Geophysical Research–Solid Earth, v. 115, p. B10103, doi:10.1029/2009JB007205.

Kirschvink, J.L., 1980, The least-squares line and plane and the analysis of paleomagnetic data: Geophysical Journal of the Royal Astronomical Society, v. 62, no. 3, p. 699–718, doi:10.1111/j.1365-246X.1980.tb02601.x.

Kirschvink, J.L., 1992, Late Proterozoic low-latitude global glaciation: The snowball Earth, *in* Schopf, J.W., and Klein, C., eds., The Proterozoic Biosphere: Cambridge, UK, Cambridge University Press, p. 51–52.

Kirschvink, J.L., Ripperdan, R.L., and Evans, D.A., 1997, Evidence for a large-scale reorganization of Early Cambrian continental masses by inertial interchange true polar wander: Science, v. 277, no. 5325, p. 541–545, doi:10.1126/science.277.5325.541.

Kirschvink, J.L., Kopp, R.E., Raub, T.D., Baumgartner, C.T., and Holt, J.W., 2008, Rapid, precise, and high-sensitivity acquisition of paleomagnetic and rock-magnetic data: Development of a low-noise automatic sample changing system for superconducting rock magnetometers: Geochemistry Geophysics Geosystems, v. 9, Q05Y01, doi:10.1029/2007GC001856.

Kruiver, P.P., Dekkers, M.J., and Heslop, D., 2001, Quantification of magnetic coercivity components by the analysis of acquisition curves of isothermal remanent magnetization: Earth and Planetary Science Letters, v. 189, no. 3–4, p. 269–276, doi:10.1016/S0012-821X(01)00367-3.

Lane, L.S., 1997, Canada Basin, Arctic Ocean: Evidence against a rotational origin: Tectonics, v. 16, no. 3, p. 363–387, doi:10.1029/97TC00432.

LeCheminant, A.N., and Heaman, L.M., 1989, Mackenzie igneous events, Canada: Middle Proterozoic hotspot magmatism associated with ocean opening: Earth and Planetary Science Letters, v. 96, no. 1–2, p. 38–48, doi:10.1016/0012-821X(89)90122-2.

Li, Z.X., Evans, D.A.D., and Zhang, S., 2004, A 90° spin on Rodinia: Possible causal links between the Neoproterozoic supercontinent, superplume, true polar wander and low-latitude glaciation: Earth and Planetary Science Letters, v. 220, no. 3–4, p. 409–421, doi:10.1016/S0012-821X(04)00064-0.

Li, Z.-X., Bogdanova, S.V., Collins, A.S., Davidson, A., De Waele, B., Ernst, R.E., Fitzsimmons, I.C.W., Fuck, R.A., Gladkochub, D.P., Jacobs, J., Karlstrom, K.E., Lu, S., Natapov, L.M., Pease, V., Pisarevsky, S.A., Thrane, K., and Vernikovsky, V., 2008, Assembly, configuration, and break-up history of Rodinia: A synthesis: Precambrian Research, v. 160, no. 1–2, p. 179–210, doi:10.1016/j.precamres.2007.04.021.

Li, Z.X., Evans, D.A., and Halverson, G.P., 2013, Neoproterozoic glaciations in a revised global palaeogeography from the breakup of Rodinia to the assembly of Gondwanaland: Sedimentary Geology, v. 294, p. 219–232, doi:10.1016/j.sedgeo.2013.05.016.

Lund, K., 2008, Geometry of the Neoproterozoic and Paleozoic rift margin of western Laurentia: Implications for mineral deposit settings: Geosphere, v. 4, no. 2, p. 429–444, doi:10.1130/GES00121.1.

Lund, K., Aleinikoff, J., Evans, K., Dewitt, E., and Unruh, D., 2010, SHRIMP U-Pb dating of recurrent Cryogenian and Late Cambrian–Early Ordovician alkalic magmatism in central Idaho: Implications for Rodinian rift tectonics: Geological Society of America Bulletin, v. 122, p. 430–453, doi:10.1130/B26565.1.

Macdonald, F.A., Schmitz, M.D., Crowley, J.L., Roots, C.F., Jones, D.S., Maloof, A.C., Strauss, J.V., Cohen, P.A., Johnston, D.T., and Schrag, D.P., 2010, Calibrating the Cryogenian: Science, v. 327, no. 5970, p. 1241–1243, doi:10.1126/science.1183325.

Macdonald, F.A., Smith, E.F., Strauss, J.V., Cox, G.M., Halverson, G.P., and Roots, C.F., 2011, Neoproterozoic and early Paleozoic correlations in the western Ogilvie Mountains, Yukon, *in* MacFarlane, K.E., Weston, L.H., and Relf, C., eds., Yukon Exploration and Geology 2010: Whitehorse, Yukon Geological Survey, p. 161–182.

Macdonald, F.A., Halverson, G.P., Strauss, J.V., Smith, E.F., Cox, G.M., Sperling, E.A., and Roots, C.F., 2012, Early Neoproterozoic basin formation in Yukon, Canada: Implications for the make-up and break-up of Rodinia: Geoscience Canada, v. 39, p. 77–99.

Macdonald, F.A., Strauss, J.V., Sperling, E.A., Halverson, G.P., Narbonne, G.M., Johnston, D.T., Kunzmann, M., Schrag, D.P., and Higgins, J.A., 2013, The stratigraphic relationship between the Shuram carbon isotope excursion, the oxygenation of Neoproterozoic oceans, and the first appearance of the Ediacara biota and bilaterian trace fossils in northwestern Canada: Chemical Geology, v. 362, p. 250–272, doi:10.1016/j.chemgeo.2013.05.032.

MacNaughton, R.B., Narbonne, G.M., and Dalrymple, R.W., 2000, Neoproterozoic slope deposits, Mackenzie Mountains, northwestern Canada: Implications for passive-margin development and Ediacaran faunal ecology: Canadian Journal of Earth Sciences, v. 37, no. 7, p. 997–1020, doi:10.1139/e00-012.

MacNaughton, R.B., Roots, C.F., and Martel, E., 2008, Neoproterozoic–(?)Cambrian Lithostratigraphy, Northeast Sekwi Mountain Map Area, Mackenzie Mountains, Northwest Territories: New Data from Measured Sections: Geological Survey of Canada, Current Research (Online) 2008-16, 17 p.

Mair, J.L., Hart, C.J., and Stephens, J.R., 2006, Deformation history of the northwestern Selwyn Basin, Yukon, Canada: Implications for orogen evolution and mid-Cretaceous magmatism: Geological Society of America Bulletin, v. 118, no. 3–4, p. 304–323, doi:10.1130/B25763.1.

Maloof, A.C., Halverson, G.P., Kirschvink, J.L., Schrag, D.P., Weiss, B.P., and Hoffman, P.F., 2006, Combined paleomagnetic, isotopic, and stratigraphic evidence for true polar wander from the Neoproterozoic Akademikerbreen Group, Svalbard, Norway: Geological Society of America Bulletin, v. 118, no. 9–10, p. 1099–1124, doi:10.1130/B25892.1.

Martel, E., Turner, E.C., and Fischer, B.J., 2011, Geology of the Central Mackenzie Mountains of the Northern Canadian Cordillera, Sewki Mountain (105P), Mount Eduni (106A), and Northwestern Wrigley Lake (95M) Map-Areas, Northwest Territories, NWT Special Volume, Volume 1: Yellowknife, Canada, Northwest Territories Geoscience Office, 423 p.

Maurin, J.C., and Guiraud, R., 1990, Relationships between tectonics and sedimentation in the Barremo-Aptian intracontinental basins of northern Cameroon, *in* Kogbe, C.A., and Lang, J., eds., African Continental Phanerozoic Sediments: Journal of African Earth Sciences, v. 10, p. 331–340, doi:10.1016/0899-5362(90)90064-L.

McElhinny, M.W., and McFadden, P.L., 1997, Palaeosecular variation over the past 5 Myr based on a new generalized database: Geophysical Journal International, v. 131, no. 2, p. 240–252, doi:10.1111/j.1365-246X.1997.tb01219.x.

McElhinny, M.W., and Merrill, R.T., 1975, Geomagnetic secular variation over the past 5 my: Reviews of Geophysics, v. 13, no. 5, p. 687–708, doi:10.1029/RG013i005p00687.

McFadden, P.L., and McElhinny, M.W., 1990, Classification of the reversal test in palaeomagnetism: Geophysical Journal International, v. 103, no. 3, p. 725–729, doi:10.1111/j.1365-246X.1990.tb05683.x.

McMechan, M.E., Thompson, R.I., Cook, D.G., Gabrielse, H., and Yorath, C.J., 1992, Structural styles: Foreland belt, *in* Gabrielse, H., and Yorath, C.J., eds., Geology of the Cordilleran Orogen in Canada: Geological Survey of Canada, Geology of Canada 4, p. 634–650.

Miller, E.L., Soloviev, A., Kuzmichev, A., Gehrels, G., Toro, J., and Tuchkova, M., 2008, Jurassic and Cretaceous foreland basin deposits of the Russian Arctic: Separated by birth of the Makarov Basin?: Norwegian Journal of Geology, v. 88, p. 201–226.

Miller, J.D., and Kent, D.V., 1988, Regional trends in the timing of Alleghanian remagnetization in the Appalachians: Geology, v. 16, no. 7, p. 588–591, doi:10.1130/0091-7613(1988)016<0588:RTITTO>2.3.CO;2.

Miller, J.M.G., 1985, Glacial and syntectonic sedimentation: The Upper Proterozoic Kingston Peak Formation, southern Panamint Range, eastern California: Geological Society of America Bulletin, v. 96, no. 12, p. 1537–1553, doi:10.1130/0016-7606(1985)96<1537:GASSTU>2.0.CO;2.

Mitchell, R.N., Kilian, T.M., Raub, T.D., Evans, D.A., Bleeker, W., and Maloof, A.C., 2011, Sutton hotspot: Resolving Ediacaran–Cambrian tectonics and true polar wander for Laurentia: American Journal of Science, v. 311, no. 8, p. 651–663, doi:10.2475/08.2011.01.

Moores, E.M., 1991, Southwest US–East Antarctic (SWEAT) connection: A hypothesis: Geology, v. 19, no. 5, p. 425–428, doi:10.1130/0091-7613(1991)019<0425:SUSEAS>2.3.CO;2.

Morris, G.A., Larson, P.B., and Hooper, P.R., 2000, 'Subduction style' magmatism in a non-subduction setting: The Colville igneous complex, NE Washington State, USA: Journal of Petrology, v. 41, no. 1, p. 43–67, doi:10.1093/petrology/41.1.43.

Morris, W.A., 1977, Paleolatitude of glaciogenic Upper Precambrian Rapitan Group and the use of tillites as chronostratigraphic marker horizons: Geology, v. 5, no. 2, p. 85–88, doi:10.1130/0091-7613(1977)5<85:POGUPR>2.0.CO;2.

Morrow, D.W., 1999, Lower Paleozoic Stratigraphy of Northern Yukon Territory and Northwestern District of Mackenzie: Geological Survey of Canada Bulletin 538, 202 p., doi:10.4095/210998.

Morrow, D.W., Cumming, G.L., and Aulstead, K.L., 1990, The Gas-Bearing Devonian Manetoe Facies, Yukon and Northwest Territories: Geological Survey of Canada Bulletin 400, 54 p., doi:10.4095/131331.

Moynihan, D., 2014, Bedrock Geology of NTS 106B/04, Eastern Rackla Belt, *in* MacFarlane, K.E., Nordling, M.G., and Sack, P.J., eds., Yukon Exploration and Geology 2013: Whitehorse, Yukon Geological Survey, p. 147–167.

Murphy, D.C., 1997, Geology of the McQuesten River region, Northern McQuesten and Mayo Map Areas, Yukon Territory (115P/14, 15, 16; 105M/13, 14): Exploration and Geological Services Division, Yukon Region, Indian and Northern Affairs Canada Bulletin 6, 122 p.

Mustard, P.S., 1991, Normal faulting and alluvial fan deposition, basal Windermere tectonic assemblage, Yukon, Canada: Geological Society of America Bulletin, v. 103, no. 10, p. 1346–1364, doi:10.1130/0016-7606(1991)103<1346:NFAAFD>2.3.CO;2.

Mustard, P.S., and Roots, C.F., 1997, Rift-Related Volcanism, Sedimentation, and Tectonic Setting of the Mount Harper Group, Ogilvie Mountains, Yukon Territory: Geological Survey of Canada Bulletin 492, 92 p., doi:10.4095/208670.

Narbonne, G.M., 1994, New Ediacaran fossils from the Mackenzie Mountains, northwestern Canada: Journal of Paleontology, v. 68, no. 3, p. 411–416.

Narbonne, G.M., and Aitken, J.D., 1990, Ediacaran fossils from the Sekwi Brook area, Mackenzie Mountains, northwest Canada: Palaentology, v. 33, no. 4, p. 945–980.

Narbonne, G.M., and Gehling, J.G., 2003, Life after snowball: The oldest complex Ediacaran fossils: Geology, v. 31, no. 1, p. 27–30, doi:10.1130/0091-7613(2003)031<0027:LASTOC>2.0.CO;2.

Narbonne, G.M., Xiao, S., and Shields-Zhou, G., 2012, Ediacaran period, *in* Gradstein, F., Ogg, J., Schmitz, M.D., and Ogg, G., eds., Geologic Timescale 2012: Oxford, UK, Elsevier, p. 427–449.

Norris, D.K., 1972, En echelon folding in the northern Cordillera of Canada: Bulletin of Canadian Petroleum Geology, v. 20, no. 3, p. 634–642.

Norris, D.K., 1985, Eastern Cordilleran foldbelt of northern Canada: Its structural geometry and hydrocarbon potential: American Association of Petroleum Geologists Bulletin, v. 69, no. 5, p. 788–808.

Norris, D.K., 1997, Geological setting, *in* Norris, D.K., ed., The Geology, Mineral and Hydrocarbon Potential of Northern Yukon Territory and Northwestern District of Mackenzie: Geological Survey of Canada Bulletin 422, Chap. 3, p. 21–64, doi:10.4095/208886.

Norris, D.K., and Dyke, L.D., 1997, Proterozoic, *in* Norris, D.K., ed., The Geology, Mineral and Hydrocarbon Potential of Northern Yukon Territory and Northwestern District of Mackenzie: Geological Survey of Canada Bulletin 422, Chap. 4, p. 65–84, doi:10.4095/208886.

Ootes, L., Gleeson, S.A., Turner, E., Rasmussen, K., Gordey, S., Falck, H., and Pierce, K., 2013, Metallogenic evolution of the Mackenzie and eastern Selwyn Mountains of Canada's Northern Cordillera, Northwest Territories: A compilation and review: Geoscience Canada, v. 40, no. 1, p. 40–69, doi:10.12789/geocanj.2013.40.005.

O'Reilly, W., 1984, Rock and Mineral Magnetism: Glasgow, UK, Blackie & Son Limited, 220 p., doi:10.1007/978-1-4684-8468-7.

Palmer, H.C., and Hayatsu, A., 1975, Paleomagnetism and K-Ar dating of some Franklin lavas and diabases, Victoria Island: Canadian Journal of Earth Sciences, v. 12, no. 8, p. 1439–1447, doi:10.1139/e75-130.

Palmer, H.C., Baragar, W.R.A., Fortier, M., and Foster, J.H., 1983, Paleomagnetism of late Proterozoic rocks, Victoria Island, Northwest Territories, Canada: Canadian Journal of Earth Sciences, v. 20, no. 9, p. 1456–1469, doi:10.1139/e83-131.

Park, J.K., 1981, Paleomagnetism of basic intrusions from the Brock inlier, Northwest Territories, Canada: Canadian Journal of Earth Sciences, v. 18, no. 10, p. 1637–1641, doi:10.1139/e81-151.

Park, J.K., 1995, Paleomagnetism of the late Neoproterozoic Blueflower and Risky formations of the northern Cordillera, Canada: Canadian Journal of Earth Sciences, v. 32, p. 718–729, doi:10.1139/e95-061.

Park, J.K., 1997, Paleomagnetic evidence for low-latitude glaciation during deposition of the Neoproterozoic Rapitan Group, Mackenzie Mountains, N.W.T., Canada: Canadian Journal of Earth Sciences, v. 34, no. 1, p. 34–49, doi:10.1139/e17-003.

Park, J.K., Roots, C.F., and Brunet, N., 1992, Paleomagnetic Evidence for Rotation in the Neoproterozoic Mount Harper Volcanic Complex, Ogilvie Mountains, Yukon Territory: Current Research, Part E: Geological Survey of Canada Paper 92-1E, p. 1–10.

Pehrsson, S.J., and Buchan, K.L., 1999, Borden dykes of Baffin Island, Northwest Territories: A Franklin U-Pb baddeleyite age and a paleomagnetic reinterpretation: Canadian Journal of Earth Sciences, v. 36, no. 1, p. 65–73, doi:10.1139/e98-091.

Pilkington, M., and Saltus, R.W., 2009, The Mackenzie River magnetic anomaly, Yukon and Northwest Territories, Canada—Evidence for early Proterozoic magmatic arc crust at the edge of the North American craton: Tectonophysics, v. 478, no. 1–2, p. 78–86, doi:10.1016/j.tecto.2008.09.006.

Pisarevsky, S.A., Wingate, M.T., Powell, C.M., Johnson, S., and Evans, D.A., 2003, Models of Rodinia assembly and fragmentation, *in* Yoshida, M., Windley, B.F., and Dasgupta, S., eds., Proterozoic East Gondwana: Supercontinent Assembly and Breakup: Geological Society of London Special Publication 206, p. 35–55, doi:10.1144/GSL.SP.2003.206.01.04.

Pisarevsky, S.A., Gladkochub, D.P., Konstantinov, K.M., Mazukabzov, A.M., Stanevich, A.M., Murphy, J.B., Tait, J.A., Donskaya, T.V., and Konstantinov, I.K., 2013, Paleomagnetism of Cryogenian Kitoi mafic dykes in south Siberia: Implications for Neoproterozoic paleogeography: Precambrian Research, v. 231, p. 372–382, doi:10.1016/j.precamres.2013.04.007.

Preeden, U., Mertanen, S., Elminen, T., and Plado, J., 2009, Secondary magnetizations in shear and fault zones in southern Finland: Tectonophysics, v. 479, no. 3–4, p. 203–213, doi:10.1016/j.tecto.2009.08.011.

Pugh, D.C., 1983, Pre-Mesozoic Geology in the Subsurface of Peel River Map Area, Yukon Territory and District of Mackenzie: Geological Survey of Canada Memoir 401, 61 p.

Pullaiah, G., Irving, E., Buchan, K.L., and Dunlop, D.J., 1975, Magnetization changes caused by burial and uplift: Earth and Planetary Science Letters, v. 28, no. 2, p. 133–143, doi:10.1016/0012-821X(75)90221-6.

Pyle, L.J., Narbonne, G.M., James, N.P., Dalrymple, R.W., and Kaufman, A.J., 2004, Integrated Ediacaran chronostratigraphy, Wernecke Mountains, northwestern Canada: Precambrian Research, v. 132, no. 1–2, p. 1–27, doi:10.1016/j.precamres.2004.01.004.

Rainbird, R.H., 1993, The sedimentary record of mantle plume uplift preceding eruption of the Neoproterozoic Natkusiak flood basalt: The Journal of Geology, v. 101, p. 305–318, doi:10.1086/648225.

Robertson, W.A., and Baragar, W.R.A., 1972, The petrology and paleomagnetism of the Coronation sills: Canadian Journal of Earth Sciences, v. 9, no. 2, p. 123–140, doi:10.1139/e72-011.

Robyn, T.L., 1979, Miocene volcanism in eastern Oregon: An example of calc-alkaline volcanism unrelated to subduction: Journal of Volcanology and Geothermal Research, v. 5, p. 149–161, doi:10.1016/0377-0273(79)90038-6.

Rohr, K.M., Lane, L.S., and MacLean, B.C., 2011, Subsurface compressional structures and facies transitions imaged by seismic reflection data, eastern margin of Richardson Trough, Peel Plateau, Yukon: Bulletin of Canadian Petroleum Geology, v. 59, no. 2, p. 131–146, doi:10.2113/gscpgbull.59.2.131.

Rooney, A.D., Macdonald, F.A., Strauss, J.V., Dudás, F.Ö., Hallmann, C., and Selby, D., 2014, Re-Os geochronology and coupled Os-Sr isotope constraints on the Sturtian snowball Earth: Proceedings of the National Academy of Sciences of the United States of America, v. 111, no. 1, p. 51–56, doi:10.1073/pnas.1317266110.

Rooney, A.D., Strauss, J.V., Brandon, A.D., and Macdonald, F.A., 2015, A Cryogenian chronology: Two long-lasting, synchronous Neoproterozoic glaciations: Geology, v. 43, no. 5, p. 459–462, doi:10.1130/G36511.1.

Roots, C.F., 1987, Regional Tectonic Setting and Evolution of the Late Proterozoic Mount Harper Volcanic Complex, Ogilvie Mountains, Yukon [Ph.D. thesis]: Northfield, Minnesota, Carleton University, 180 p.

Root, K.G., 1987, Geology of the Delphine Creek Area, Southeastern British Columbia: Implications for the Proterozoic and Paleozoic Development of the Cordilleran Divergent Margin [Ph.D. thesis]: Calgary, Canada, University of Calgary, 446 p.

Ross, G.M., 1991, Tectonic setting of the Windermere Supergroup revisited: Geology, v. 19, no. 11, p. 1125–1128, doi:10.1130/0091-7613(1991)019<1125:TSOTWS>2.3.CO;2.

Schlische, R.W., 1995, Geometry and origin of fault-related folds in extensional settings: American Association of Petroleum Geologists Bulletin, v. 79, no. 11, p. 1661–1678.

Schlische, R.W., 2003, Progress in understanding the structural geology, basin evolution, and tectonic history of the eastern North American rift system, *in* LeTourneau, P.M., and Olsen, P.E., eds., The Great Rift Valleys of Pangea in Eastern North America: Volume 1. Tectonics, Structure and Volcanism: New York, Columbia University Press, p. 21–64.

Schwab, D.L., Thorkelson, D.J., Mortensen, J.K., Creaser, R.A., and Abbott, J.G., 2004, The Bear River dykes (1265–1269 Ma): Westward continuation of the Mackenzie dyke swarm into Yukon, Canada: Precambrian Research, v. 133, no. 3–4, p. 175–186, doi:10.1016/j.precamres.2004.04.004.

Sears, J.W., and Price, R.A., 1978, The Siberian connection: A case for Precambrian separation of the North American and Siberian cratons: Geology, v. 6, no. 5, p. 267–270, doi:10.1130/0091-7613(1978)6<267:TSCACF>2.0.CO;2.

Sears, J.W., and Price, R.A., 2003, Tightening the Siberian connection to western Laurentia: Geological Society of America Bulletin, v. 115, no. 8, p. 943–953, doi:10.1130/B25229.1.

Sharp, I.R., Gawthorpe, R.L., Armstrong, B., and Underhill, J.R., 2000, Propagation history and passive rotation of mesoscale normal faults: Implications for synrift stratigraphic development: Basin Research, v. 12, no. 3–4, p. 285–305, doi:10.1046/j.1365-2117.2000.00132.x.

Shephard, G.E., Müller, R.D., and Seton, M., 2013, The tectonic evolution of the Arctic since Pangea breakup: Integrating constraints from surface geology and geophysics with mantle structure: Earth-Science Reviews, v. 124, p. 148–183, doi:10.1016/j.earscirev.2013.05.012.

Smith, E.I., Feuerbach, D.L., Naumann, T.R., and Mills, J.G., 1990, Mid-Miocene volcanic and plutonic rocks in the Lake Mead area of Nevada and Arizona; production of intermediate igneous rocks in an extensional environment, *in* Anderson, J.L., ed., The Nature and Origin of Cordilleran Magmatism: Geological Society of America Memoir 174, p. 169–194, doi:10.1130/MEM174-p169.

Stewart, J.N., 1972, Initial deposits of the Cordilleran geosyncline: Evidence for a late Precambrian (850 m.y.) continental separation: Geological Society of America Bulletin, v. 83, no. 5, p. 1345–1360, doi:10.1130/0016-7606(1972)83[1345:IDITCG]2.0.CO;2.

Stokking, L. B., and Tauxe, L., 1990, Properties of chemical remanence in synthetic hematite: Testing theoretical predictions: Journal of Geophysical Research–Solid Earth (1978–2012), v. 95, no. B8, p. 12,639–12,652.

Strauss, J.V., Rooney, A.D., Macdonald, F.A., Brandon, A.D., and Knoll, A.H., 2014a, 740 Ma vase-shaped microfossils from Yukon, Canada: Implications for Neoproterozoic chronology and biostratigraphy: Geology, v. 42, no. 8, p. 659–662, doi:10.1130/G35736.1.

Strauss, J.V., Roots, C.F., Macdonald, F.A., Halverson, G.P., Eyster, A., and Colpron, M., 2014b, Geological Map of the Coal Creek Inlier, Ogilvie Mountains (NTS 116B/10-15 and 116C/9,16): Yukon Geological Survey Open-File 2014-15, scale 1:100,000.

Strauss, J.V., Macdonald, F.A., Halverson, G.P., Tosca, N.J., Schrag, D.P., and Knoll, A.H., 2015, Stratigraphic evolution of the Neoproterozoic Callison Lake Formation: Linking the break-up of Rodinia to the Islay carbon isotope excursion: American Journal of Science, v. 315, p. 881–944, doi:10.2475/10.2015.01.

Tauxe, L., and Watson, G.S., 1994, The fold test: An eigen analysis approach: Earth and Planetary Science Letters, v. 122, no. 3–4, p. 331–341, doi:10.1016/0012-821X(94)90006-X.

Tauxe, L., Butler, R.F., Van der Voo, R., and Banerjee, S.K., 2010, Essentials of Paleomagnetism: Berkeley, California, University of California Press, 489 p.

Tempelman-Kluit, D.J., 1970, Stratigraphy and structure of the 'Keno Hill Quartzite' in Tombstone River–Upper Klondike River Map Areas, Yukon Territory (116B/7,B/8): Geological Survey of Canada Bulletin 180, 103 p., 2 maps at scale 1:506,880 and scale 1:63,360.

Thompson, R.I., Roots, C.F., and Mustard, P.S., 1994, Geology of Dawson Map Area (116B, C, Northeast of Tintina Trench): Geological Survey of Canada Open-File 2849, scale 1:50,000, doi:10.4095/194830.

Thorkelson, D.J., 2000, Geology and Mineral Occurrences of the Slats Creek, Fairchild Lake and "Dolores Creek" Areas, Wernecke Mountains (106D/16, 106C/13, 106C/14), Yukon Territory: Exploration and Geological Services Division, Yukon, Indian and Northern Affairs Canada Bulletin 10, 73 p.

Thorkelson, D.J., Abbott, J., Mortensen, J., Creaser, R., Villeneuve, M., McNicoll, V., and Layer, P., 2005, Early and Middle Proterozoic evolution of Yukon, Canada: Canadian Journal of Earth Sciences, v. 42, no. 6, p. 1045–1071, doi:10.1139/e04-075.

Torsvik, T.H., Van der Voo, R., Preeden, U., Mac Niocaill, C., Steinberger, B., Doubrovine, P., van Hinsbergen, D.J.J., Domeier, M., Gaina, C., Tohver, E., Meert, J.G., McCausland, P.J., and Cocks, L.R.M., 2012, Phanerozoic polar wander, palaeogeography and dynamics: Earth-Science Reviews, v. 114, no. 3–4, p. 325–368, doi:10.1016/j.earscirev.2012.06.007.

Turner, E.C., 2011, Stratigraphy of the Mackenzie Mountains Supergroup in the Wernecke Mountains, Yukon, *in* MacFarlane, K.E., Weston, L.H., and Relf, C., eds., Yukon Exploration and Geology 2010: Whitehorse, Yukon, Canada, Yukon Geological Survey, p. 207–231.

Turner, E.C., and Long, D.G.F., 2008, Basin architecture and syndepositional fault activity during deposition of the Neoproterozoic Mackenzie Mountains Supergroup, Northwest Territories, Canada: Canadian Journal of Earth Sciences, v. 45, no. 10, p. 1159–1184, doi:10.1139/E08-062.

Van der Voo, R., 1990, The reliability of paleomagnetic data: Tectonophysics, v. 184, no. 1, p. 1–9, doi:10.1016/0040-1951(90)90116-P.

Watson, G.S., 1956, A test for randomness of directions: Geophysical Supplements to the Monthly Notices of the Royal Astronomical Society, v. 7, no. 4, p. 160–161, doi:10.1111/j.1365-246X.1956.tb05561.x.

Watson, G.S., 1983, Large sample theory of the Langevin distributions: Journal of Statistical Planning and Inference, v. 8, no. 3, p. 245–256, doi:10.1016/0378-3758(83)90043-5.

Witte, W. K., and Kent, D. V., 1991, Tectonic implications of a remagnetization event in the Newark Basin: Journal of Geophysical Research–Solid Earth (1978–2012), v. 96, no. B12, p. 19,569–19,582.

Wynne, P.J., Enkin, R.J., Baker, J., Johnston, S.T., and Hart, C.J., 1998, The big flush: Paleomagnetic signature of a 70 Ma regional hydrothermal event in displaced rocks of the northern Canadian Cordillera: Canadian Journal of Earth Sciences, v. 35, no. 6, p. 657–671, doi:10.1139/e98-014.

Yeo, G.M., 1984, The Rapitan Group: Relevance to the Global Association of Late Proterozoic Glaciation and Iron-Formation [Ph.D. thesis]: London, Ontario, Canada, University of Western Ontario, 599 p.

Yonkee, W.A., Dehler, C.D., Link, P.K., Balgord, E.A., Keeley, J.A., Hayes, D.S., Wells, M.L., Fanning, C.M., and Johnston, S.M., 2014, Tectono-stratigraphic framework of Neoproterozoic to Cambrian strata, west-central US: Protracted rifting, glaciation, and evolution of the North American Cordilleran margin: Earth-Science Reviews, v. 136, p. 59–95, doi:10.1016/j.earscirev.2014.05.004.

Yorath, C.J., 1992, Upper Jurassic to Paleogene assemblages, *in* Gabrielse, H., and Yorath, C.D., eds., Geology of the Cordilleran Orogen in Canada: Geological Survey of Canada, Geology of Canada 4, p. 331–371.

Young, G.M., 1995, Are Neoproterozoic glacial deposits preserved on the margins of Laurentia related to the fragmentation of two supercontinents?: Geology, v. 23, no. 2, p. 153–156, doi:10.1130/0091-7613(1995)023<0153:ANGDPO>2.3.CO;2.

Young, G.M., Jefferson, C.W., Delaney, G.D., and Yeo, G.M., 1979, Middle and Upper Proterozoic evolution of the northern Canadian Cordillera and Shield: Geology, v. 7, no. 3, p. 125–128, doi:10.1130/0091-7613(1979)7<125:MALPEO>2.0.CO;2.